

See discussions, stats, and author profiles for this publication at: <https://www.researchgate.net/publication/356972251>

A new, experimental path to nucleosynthesis

Preprint · December 2021

DOI: 10.13140/RG.2.2.31880.75527

CITATIONS

0

READS

710

1 author:



Jürg Wyttbach

Independent

5 PUBLICATIONS 4 CITATIONS

SEE PROFILE

Some of the authors of this publication are also working on these related projects:



Low energy nuclear reactions [View project](#)



Nuclear and particle physics 2.0 (new SO(4) physics) [View project](#)

A new, experimental path to nucleosynthesis

Jürg A. Wyttenbach, Russ George Atom-Ecology

Abstract

Nucleosynthesis is far from being understood. The main reason is that physics has a poor working model for dense matter. The other reason: New paths[1][2][3][4][5], since 30 years at least, have been systematically ignored as each would have challenged running projects like ITER, CERN.

In 1989 two electro-chemists announced a breakthrough new process[1] called cold fusion(LENR****). Within hours a world wide tsunami wave of excitement flooded the news channels and many laboratories immediately started a replication experiment to verify the claims. The first that did have success was a US military lab, that for obvious reasons did not publish it. Others failed due to lack of knowledge or for foul play reasons.

As we will show here, the so called “cold fusion reactions” may well explain a huge chunk of nucleosynthesis. Together with Holmlid’s experimental findings, that ^4He can be produced without neutrons, just from Hydrogen and the fact that hydrogen can undergo a stable weak nuclear bond[6][7], we now can explain some of what potentially happens since billions of years in the earths mantle and core.

Deuterium is more abundant in comet’s water than on earth. Why and how this could happen is explained by our experimental, rare earth powder mixtures, that all consist of classically “stable” elements loaded with Deuterium. These powders, in some cases, start to produce well known, because predictable, gamma radiation even at room temperature and without any stimulation, while consuming Deuterium! We here, in the first part, will discuss some spectra we recorded in late October 2018 and then look at some theoretical aspects of cold fusion needed to explain gamma spectra.

****LENR stays for Low Energy Nuclear Reactions. New physics will be presented in a separate paper.

1 Introduction

Over - now decades - researchers tried, within existing paradigm, to isolate the basic factors that drive a LENR reaction. So far all failed because one key criterion never got enough attention. How can we measure the physics behind LENR? Unluckily contemporary physics, the standard model (SM), has no answer. Russ George, a LENR researcher for three decades [7] [8], that visited and worked in many labs in different continents has acquired some unique experience of fuel preparation. Russ’s latest approach, as a Biologist, (and “born” experimental physicist) was novel as he did ask himself: “Why not try to use a mixture of metal powders that are magnetic? Can it be that LENR needs a kind of ecosystem to reproduce cold fusion with a high success percentage?” This approach proved very fruitful and has some real world backing. What is the driving force behind volcanism? Even on distant, small planets like Pluto? Why has planet earth less Deuterium than found in comets? First results simply triggered a Geiger counter. Here the second story started. Jürg A. Wyttenbach, about now 4 years ago, started to reason about a new physics model (now called SO(4) physics[7] or short SOP) for dense matter, that could be used to describe cold fusion. At the time of the first Geiger bursts the model already successfully resolved the proton structure and it was obvious that new physics must be **based on magnetism** only. Magnetic mass-like interaction is based on resonance. This is well known from antenna physics and also holds for all EM mass like interactions.

The simple formula:

$$(1) E_{\text{PotBohr}} = m_e * \alpha^2! \quad (m_e \text{ in eV!})$$

shows that the Bohr potential does not depend on charge and the Bohr radius. In fact we can give the 10 digits exact ionization energy of Hydrogen via SOP using a coupled magnetic mass-resonance relation. This formula (1) is the (1 x 1) magnetic resonance energy of the electron in the classic 3D,t frame and needs to be corrected by $\frac{1}{2}$ for the SO(4) frame.

$$(2) E_{\text{potDBR}} = m_p * (\alpha/2\pi)$$

A similar resonance is known from the proton (see formula 2) where we get the proton De Broglie(dbr) radius potential at $r_{\text{pdbr}} = 0.841235640192 \text{ fm}$ (=4x classic **dbr** due to SO(4) metric change) when we multiply the proton mass with the force factor $(\alpha/2\pi)$ we in SOP call 2FC’. This factor is important for nuclear bonds. r_{pdbr} is one of the two proton magnetic resonance radius.

1.1 First results

In the next step of the experiment, a gamma spectrometer the first time revealed the true nature of LENR. The fuel probes, based on a powder mixture of magnetic elements loaded with Deuterium have been placed and sealed inside a ceramic tube. Within hours we could understand, as expected from the model, that many so called “magnetic gamma lines” could be seen. All this happened in a laboratory that most would call grandmother’s kitchen. The investment was lifetime experience in lab work and deep understanding of physics rather than big money. A magnetic gamma line is emitted from a gamma state that also expresses a magnetic moment. The basic

assumption was, that for fusion to be understood, it is key to understand how the energy is removed or transported. If no kinetic momentum - e.g. an off flying electron/proton/neutron - is available to attach excess energy, then the **classic kinetic fusion paths are forbidden**. Isotopes that own a magnetic gamma state can work like antennas and are able to accept a large junk of fusion energy. Direct downscaling of fusion energy to phonon level is not allowed due to - classically said - multiple changes of "frame of reference". Of course, as a first result, the factual existence of magnetically induced coupling gamma states (lines) did already confirm that all nuclear mass is equivalent to EM-flux.

1.2 Gamma spectroscopy

In a clean, well shielded lab gamma spectroscopy normally is used to track the lines of radioactive decay, either a natural one or an induced one. The lines to be seen - usually a small set - can be exactly predicted by the experimental setup. Further it is well known which lines do occur according to the tabulated IAEA [10] probabilities. In LENR research so far nobody has published discrete spectra of a reaction. We only know one paper[11] that shows a long time measured gamma spectral region with an increased count near the ^{137}Cs 662keV calibration line. We here for the first time will present spectra of a cold fusion reaction, that do show a wide range of gamma lines, that finally do explain how LENR works. At first sight our measurements did look like chaos and only the painful work of going down to histogram/channel level allowed a useful interpretation. As a consequence we had to develop a new analyzing method that could deal with broad range/ large number (> 300) of different lines above background. Doing this manually is possible for a single spectrum and some key lines, but for hundreds (spectra & lines) we had to develop new software. Finally one year after the first break-through measurement everything was in place. In a highly active fuel up to 80 lines are more than a factor of two above background. The strongest lines more than 10 fold. (This in reality is much higher as e.g. already the quartz & ceramic case (about 3mm total wall strength and the fuel powder) holding the powder blocks up to 50% of all radiation below 100keV. The "cheap" NaI spectrometer setup (gamma spectacular + Theremino software) we used, could be very well calibrated in the range of 20..300keV and also up to 662keV. We did so by using the lines of 241-Americium and 137-Cesium we also could use the 214-Pb line and some thorium lines from the lab background. The NaI sensor has been shielded by 3 cm thick rolled lead to cut down the very active background by a factor of 2.5. As we know all the elements in the fuel and did tabulate the theoretically expected lines, we can do very good matches, that only get disturbed by the very noisy lab background. All results here are double checked against two different types of background to avoid temporary transparency effects with false positive/negative signals. Long run backgrounds cannot be use to discriminate lines as possible bursts are hidden.

To ensure that the spectra and the background do match we checked that all strong background lines are also high in the measured spectrum. This is only possible with the direct view experiment background. Up to 300keV we could not detect any non random difference. Between 300..600keV we found some background peaks that later have been split into the two neighbor buckets. This is also no problem as this indicates that the line did not shift. It only shows that the electronics sometime did a slightly better discrimination.

1.3 What is cold fusion/LENR?

The term cold fusion has first been used in the 1989 presentation of Pons & Fleischmann [1]. The notion is that in cold fusion two nuclei at rest, which signifies **zero kinetic input energy**, do fuse. Generally all fusion processes that need a low input energy of e.g. less than 100eV can be termed cold fusion or low energy nuclear reactions (LENR). Fusion processes needing > 1keV input energy are well described in the literature and are called hot fusion. Usually the input energy is also related to thermic energy, what gives a temperature equivalent for the fusion event that for most LENR reaction typically is less than 1200C and for hot fusion typically is > 10 million. C. But such definitions are of no use as the cold fusion rate only indirectly depends on temperature.

In fact, classic research most of the time did focus on kinetic fusion, what defines a complete different physics, than needed for LENR. In kinetic fusion excess energy is removed by kinetic particles, whereas as in cold fusion momentum conservation excludes kinetic particles (with few exceptions). Furthermore in kinetic fusion charged particles produce strong secondary fields, which leads to the claimed so called Coulomb barrier, that factually is inexistent for cold fusion. One key for understanding cold fusion is to have a good picture of the energy removal process. Contrary to the fringe classic claim of a coulomb barrier that blocks fusion, in reality there is a barrier that blocks the energy release of fusion. A coulomb barrier is only seen in kinetic fusion due to Biot-Savart interaction of charged particles. Neutral particles at rest follow the law of magnetism as given by SO(4) physics[7]. If two magnetic masses of the same size and topology are close, then these can go into resonance, which leads to an attractive force given by flux compression. Resonance means the two EM masses engage in a new shared rotation that induces topological charge. This logically looks the same as in general relativity, where an increase in space-time curvature is equivalent to a force.

1.4 What has been known so far

Magnetic Hydrogen - a precursor of cold fusion - has first been detected by R. Santilli[2] and recently exactly measured by R. Mills[6]. Less exact measurements were made by L. Holmlid[3], where larger fragments of H^*/D^* did interact and spoil the measurement. We here call dense Hydrogen H^*/D^* . D for deuterium H for Hydrogen. H^*-H^* is the basic condensation

step of two protons, what is the prelude of fusion. H^*-H^* is a stable **nuclear molecule**, whereas as D^*-D^* ultimately will fuse to 4He and hence is metastable. There is absolutely no Coulomb-barrier that blocks the formation of H^*-H^* . The only prerequisite is a strong magnetic ordering force – provided by a so called catalyst surface, see Holmlid[12] or a strong field of an electric arc Mills[6], Klimov[13] – that forces proton spins to exactly align. This first condensation step releases about 500eV for one H^*-H^* pair (exact calculation in [7]). In fact cold fusion is the dominating process in the universe and thus the hot fusion logic of classic standard model physics is the biggest misunderstanding of cosmology. It is thus no surprise, that the new SO(4) physics model exactly can show why the classic understanding /interpretation of experiments did lead to only marginal models (QED, QCD,LQCD) that help to tailor kinetic experiments only. The so called ‘refutation’ of cold fusion by standard model physics is, historically seen, a Phlogiston-based defences rationalizing the findings of Lavasier. Classic SM physics is based on point axioms for charge, electron and on a “blubber” called mass with unknown physical properties. Further the mathematics (group structure base) used for the field only model of **mass interaction** is provably incomplete and not able to properly model communicating objects (particles). This proof is well known in computation theory and the handling of communicating processes = interacting structured masses.

1.5 What Hypotheses did we want to test?

We here will also call the powder mixture of isotopes, we use for a LENR reaction, a fuel.

- Which reactions do run in a cold fusion process?
- How can we best start reactions/ activate fuels?
- Can we isolate reaction paths from a spectrum?
- Are spectra correlated with temperature?
- Will the spectra vary with time?
- Will we see effects of new physics?

1.5.1 SO(4) physics Prediction made

From the SO(4) physics model, we did predict that the only possible “short-time” down-scaling path for the 23.8MeV D-D pre-fusion excess energy, will be magnetic coupling to so called magnetic gamma states.

We also predicted that the magnetic moment of the proton can undergo a quantization and that the so called “neutron resonance waves” must be visible in the spectra. We also predicted that a strong unidirectional magnetic field will stabilize the reaction [14].

1.6 Experimental setup

Basically we did use a simple affordable setup with the following components:

- Rare earth powders enriched with other magnetic elements (Ag,Pd,Ni,Co,W) have been loaded with deuterium.
- The powder then was filled in ceramic tubes and sealed with a high temperature quartz cement.
- Together with two tube shielded thermo couple sensors the fuel tube was placed inside a larger quartz tube.
- On the outside of the quartz tube we did wind a coil, made from Iconell wire. The winding was sparse enough to not additionally block the radiation. The coil also served as a heater and produced a directed magnet field.
- A third TC was placed outside the tube for heating control.
- The quartz tube/coil then was placed inside an ALU 'cement bricks' tube shape like reactor with an outside isolation. On one side of the bricks we had a small radiation window.
- The fuel then was activated by a heating protocol that did include several heating steps followed by so called cool downs.
- On top of each furnace a highly sensitive (> 200c/s) Russian Geiger counter has been placed.

The operation of the furnace was simple. A PID could be preset with a temperature and controlled the heating. Three thermocouples were logged by national instrument based electronics and software. Data has been recorded in seconds intervals where as the PID used 1/100" steps for calculating the adjusted current.

Excess heat production was evaluated by calibrated cool downs. For this purpose we did heat the furnace (reactor) to a constant temperature and measure the input energy needed to precisely holding the temperature. If e.g. a cool down for 3 degrees takes 1 minute but with active fuel 2 minutes then the excess energy produced within 2 minutes is on par with the calibrated energy (for 1 minute). Basically this was a screening setup only with no intention to do exact calorimetry.

1.7 Goals of the project

The initial goal of Russ George was to find a method to produce productive fuels that show a significant amount of excess heat. After some reliable geiger excess counts did occur a spectrometer was added to the setup. So a simple screening experiment changed to a deep scientific exploration. Here the author joined the team. So the final goal now is to exactly understand the physics of LENR.

1.8 Summary of findings

The best powders did deliver at least 20 Watts/ccm for at least a minute - at the optimal temperature. During a cool down multiple production points (highly stable temperatures) could be seen. Typical fuels did show 30% excess gamma counts.

The one fuel we will discuss here was by far the most active. Initially it did show 40% excess counts above background. But after a cycling around the optimal temperature the counts increased to about double the background. This optimal point has been found based on the predicted neutron wave coupling, that causes some strange shifts in the background peak region

2 Results of spectroscopy

In figure 1. below we present a delta background spectrum of a LENR reaction at two different temperatures. Usually the range between 20..300 keV is the most active one. It is easy to see that these two extracts look very similar, what indicates that the overall reaction process must be the same. But if you understand gamma spectroscopy then you know that gamma lines usually are very precise and a peak does not spawn dozens of keV. We did use a bin resolution of 600 eV for the first 200keV what should be enough to classify the lines of interest. All spectra did run for 10 minutes.

Here more than 300 lines are active - high above the background - at the "same" time and some are overlapping or pretty close. So only an inspection of the histogram file finally can tell the truth. The red line is a reminder of the peaks we tracked.

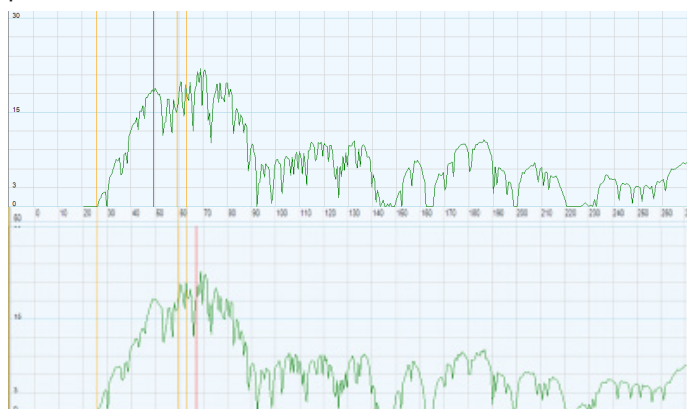


Fig.1. top spectrum at 250C, bottom at 380C – delta background in low 20..270keV range.



Fig.2 shows a typical noisy 10' uni directional lab background behind the experiment with an average count rate of 11.6c/s.

The background in view of the experiment was somewhat reduced by the containment and delivered 10.4c/s. The detector was wrapped into about 3 cm thick rolled lead sheets to suppress at least 80% of the space angle. From Fig. 1,2 you immediately can see that the background peak and the most active LENR regions do strongly overlap. This might be one reason why others couldn't

isolate any relevant signal

Fig.2 Typical lab background

The lab walls are made of old British brick stones with a high Thorium/Uranium content. The most active discrete lines we see in the background are ^{234}Th (from ^{238}U decay) lines at 63.3,92.4,92.8keV and the follow-up decay lines of ^{234}Pa . Also ^{235}U is quite dominant at 109.16, 185.7keV together with the follow up lines of ^{231}Th . The rest should be breaking radiation from the usual sources including stopped alphas.

Fig. 3 shows a large set of the most active magnetic lines we initially did search for. The column tagged "above" shows the counts above background (column "bg" is the count of the background). All these lines show at least a signal to noise ratio of 3:1.

Some lines of Fig.3 are from unstable isotopes that are produced by the reaction. Later we will explain the lines of the Samarium complex.

Fig. 3 also answers the question which elements we did use. Some of the elements were contained as minor parts e.g. in Pd or W or have been activated/produced by the reaction (e.g. ^{113}Cd).

	N+Z	Line	above	bg.		N+Z	Line	above	bg
Te	125	19800	11	0	Tm	169	193150	13	2
Tm	169	20752	6	0	Er	168	198241	14	6
Gd	155	21035	12	0	Te	125	204138	10	1
Yb	171	22000	7	0	Er	164	208080	9	2
Sm	149	22510	8	0	Yb	172	208305	11	4
Ce	140	24595	13	1	Te	125	227891	6	1
Dy	161	25651	8	0	Gd	155	239300	10	2
Sm	151	25710	8	0	Yb	171	256650	9	3
Gd	155	26531	7	2	W	183	259480	8	2
Yb	171	27100	14	1	Cd	109	259740	8	2
Pr	141	28900	16	2	Gd	156	262589	6	1
Ce	138	31900	19	8	Yb	171	262700	6	1
Sm	151	35130	15	1	Tm	169	269400	10	1
Pd	105	38720	16	1	Gd	152	271100	11	1
Sm	151	39010	25	6	Yb	173	272105	9	2
Ag	109	44770	15	4	Yb	172	272310	7	3
W	183	52595	25	9	Er	168	272876	7	3
Gd	157	54536	32	9	Sm	152	275410	9	2
Gd	155	60009	78	30	Pd	105	280410	9	3
Sm	151	61010	30	14	Er	166	280464	9	3
Te	125	61850	36	15	Cd	113	285300	10	4
Rh	103	62410	48	16	Pr	141	302600	10	3
Te	125	109276	18	8	Er	166	304910	5	2
Tm	169	109779	20	5	Tm	169	305200	5	2
Gd	155	122548	15	6	Sm	150	305680	9	1
W	183	139200	16	6	Pd	105	319140	9	3
Gd	155	141900	13	4	Ag	107	324810	11	2
Yb	171	170732	15	7	Ag	107	330000	9	2
Cd	111	171280	23	3	Tm	169	336600	10	1
Yb	173	171393	23	3	Sm	152	340450	7	1
Tm	169	177213	12	5	Gd	252	344380	9	2

Fig.3. Some highly active lines at 380C

2.1 What are magnetic lines?

The 423.15keV state of ^{107}Ag Fig.4 has three decay paths where all intermediate states do express a magnetic moment. If gamma radiation occurs, - of a line with an associated magnetic moment-, then we call it a magnetic line.

Isotope	Gamma-level	energy1	Target Line Energy	moment
107Ag	0	0.00		-0.11357
107Ag	93.125	93.12	0	4.398
107Ag	324.81	324.81	0	0.94
107Ag	423.15	423.15	0	1.03
107Ag	423.15	98.20	324.81	1.03
107Ag	423.15	330.00	93.125	1.03

Fig.4 ¹⁰⁷Ag magnetic decay

Thus all lines in Fig. 4 “are magnetic lines”. We know that also non magnetic lines can show the same behavior if they are followup lines of magnetic lines. The main reason to first check the magnetic lines was to confirm that in fact we see lines of stable isotopes that finally, indirectly get activated by low level phonon stimulation (heating) that induces fusion.

The filter used for Fig. 3 (2x above background >3x background count) does not work very well for lines inside the top peak of the background. If we go to the histogram files (at different temperature) then total counts above background shows e.g. that the ¹⁰⁷Ag 93.1keV line is only between 5..11 counts above background, which is the same count range seen from the precursor 330keV lines (Fig.3).

We will later see that fully magnetic decays are able to **internally downscale** higher states energy!

2.1.1 Why do we see gamma lines at all?

¹⁰⁷Ag is a stable isotope! Why should it send out gamma radiation? There are two possibilities. Either ¹⁰⁷Ag is formed by the fusion of ¹⁰⁵Pd + ²H, - this in fact happens as we will explain below -, or it directly converts/downscales ²H* - ²H* → ⁴He fusion energy. If e.g. ¹⁰⁷Ag would be the end point of a fusion reaction, then we should see all lines below the Q-factor of the nearest unstable nucleus. But this was, for ¹⁰⁷Ag, not the case. As we will show bellow the reaction A + ²H → B + ²H → C → A + ⁴He is the main driving factor in a highly productive powder. The net Q factor relative to B,C usually is between 2-3 MeV only as the main fusion energy is coming from ²H* - ²H* → ⁴He. But some e.g. Samarium isotopes effectively do show a full 10MeV fusion related decay. Whether this is an effect of a weak bond between the final A + ⁴He that triggers the gamma states or a result of added ²H we could not distinguish. One interesting point you may see from comparing Fig.3,4,5: The ¹⁰⁷Ag 98.2 keV line is not strongly present albeit the decay path is active. The correct question has to be asked the other way round. Why do we see some lines at all ?

We assume that due to magnetic coupling between the pre-fusion state of D*-D* e.g. the 423.15keV state of ¹⁰⁷Ag is not able to decay because a part of it's energy is bound with the D*-D* state. Thus the gamma threshold is not met. Further the 93.125keV state of ¹⁰⁷Ag is very long living (44.3 seconds). It looks like such long living state act like mediators between higher energy states an the ground state that directly can interact with the shell electrons.

Even more important is the difference in polarization (4.398) between the 93.125keV state of ¹⁰⁷Ag and the ground state (-0.11357 – 0 eV). This polarity change of the magnetic moment is crucial to stimulate strong phonon and hyper-fine coupling radiation. Induced coupling

charge is proportional to a change in magnetic flux.

See below fig. 5b. ¹⁵⁵Gd has only one almost fully magnetic decay path, marked in red, first column starting at 729.6keV. The last line (60keV Fig.3) shows a very high count above background. Also 86.059keV before is strongly elevated. The intermediate 141.9keV line most likely shows up

Elem.	A	LineEnergy	count above	Bg
Sm	151	62910	33	20
Trm	169	63120	61	43
Gd	157	63929	37	21
Sm	151	64880	26	20
Ni	61	67412	32	26
Ce	140	69500	31	26
Sm	151	69703	31	26
Nd	145	72500	36	24
La	138	72570	36	24
Rh	103	72600	36	24
Dy	164	73392	28	32
Dy	161	74566	14	22
Gd	160	75260	30	18
Sm	151	76220	14	20
Yb	174	76471	14	20
Yb	173	78647	20	46
Er	168	79804	21	58
Er	166	80578	16	22
Sm	154	81981	34	19
W	183	82918	26	37
Gd	155	86059	13	19
Gd	155	86548	22	34
Gd	156	88970	11	10
Cd	111	96750	10	13
Ag	107	98200	8	11
Sm	151	100020	13	9
Sm	151	101930	10	12
W	183	101934	10	12
W	183	102481	14	13
Gd	155	105636	18	12
Ce	136	105700	18	12
W	183	107931	16	13
Ce	138	109000	28	26

(Fig.3) because there is an other line (not shown here) following the 393.5keV state with a very close/overlapping energy (141.9 keV), that we measure with about the seen excess count.

The light blue marked decay path in column 2 show is less prominent but has many follow-up lines that end on non magnetic states. Where the path ends on a non magnetic state we prominently see (21keV,122.5keV) higher counts than seen in fully magnetic line transitions.

Fig 5a Lines inside background peak > 50% above bg. at 380C.

E state	E line	E target	moment
0			-0.25723
60.0108	60.0086	0	*
86.5468	26.531	*60.0108	-0.525
86.5468	86.5479	0	-0.525
107.5806	21.035	86.5468	*
117.9986	10.4183	*107.5806	*
117.9986	31.444	86.5468	*
117.9986	57.989	*60.0108	*
146.0696	86.0591	*60.0108	*
146.0696	146.071	0	*
214.3511	106.771	107.5806	*
230.1286	112.131	*117.9986	*
230.1286	122.548	107.5806	*
251.7056	105.636	*146.0696	1.2
251.7056	133.7	*117.9986	1.2
251.7056	191.691	*60.0108	1.2
392.317	140.61	251.7056	1.5
392.317	246.253	*146.0696	1.5
392.317	284.8	107.5806	1.5
453.67	223.6	*230.1286	*
453.67	239.3	*214.3511	*
534.3	141.9	392.317	1.9
534.3	282.6	251.7056	1.9
534.3	304.2	230.1286	1.9
729.6	195.4	534.3	2.6
729.6	337.3	392.317	2.6
729.6	515.3	214.3511	2.6
896.9	167.40	729.6	2.2
896.9	362.80	534.3	2.2
896.9	443.20	*453.67	2.2

From Fig.5b it is already clear that a single element like ¹⁵⁵Gd already can express dozens of potential lines!After a first iteration with magnetic lines only, we still had more than half of the high above background peaks unexplained. Thus in a next step we did focus on cascading lines, that can deliver irrefutable proof of the acting element/isotope. It is highly unlikely to see 6 and more followup lines just from a random spectrum at 100% counts above background.

Fig 5b. Lines inside background peak > 50% above bg. at 380C.

2.1.2 How do we identify the lines?

To identify a single line the nearest bucket line $\pm 300V$ has been exclusively used. This sometimes (just a few cases) results in two bucket hits in case we have 600eV space buckets. It is also a more hard condition for lines above 300keV where the Theremino bucket spacing did increase to 900eV. A more serious problem are lines above 500keV as the precision of the sensor can slightly vary with temperature. So in many cases, where we did manual lookup, we used 2 adjacent buckets of the target bucket to check for a significant difference to background or vice versa.

Fig 5b. Some ^{155}Gd decay paths

The use of two different backgrounds, a high one with no front shield and one in face of the experiment with 10% less counts was very helpful in avoiding false positive lines. Nevertheless if the counts did go down to 5 (e.g. with background counts = 1,2) we had to use other spectra at different temperatures to see if the line in the experiment is always present. Further most lines above 300 keV are affected by Compton scattering which might explain some excess energy in certain lower regions and also the lack of seeing many higher energy ($> 500\text{keV}$) lines. The energies below 50 keV are also elevated due to k-shell X-rays that can occur after adding ^2H to an isotope.

So there are clear criteria:

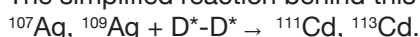
- Lines $> 3x$ background
- Lines $2-3x$ background
- Lines in counts $> 50\%$ backup and $\Delta \geq 8$
- lines $2-3x >$ background and Δ count $4-7$
- similar count but 10 counts above background
- possible lines with a too low count/ Δ just as an indication.

The first 4 criteria deliver stable results if different (not averaged) background spectra are used.

2.2 Why do these lines occur?

There are two basic fusion mechanism that produce these lines shown in Fig.3 to 6. The vast majority of the active lines is given by down-scaling of the $\text{D}^*-\text{D}^* \rightarrow ^4\text{He}$ (23.8MeV) fusion energy. But Deuterium (D^*-D^*)/Hydrogen (H^*-H^*) can also be added to almost all isotopes ($\text{A}+\text{D}^*$) and most of the time, after an intermediate state, a stable new isotope is formed. In Fig. 3 we also tabulated the ^{111}Cd and the ^{113}Cd lines. Both elements are not in our initial mixture albeit these do support LENR as the magnetic momentum structure of Cadmium is similar to Silver. These isotopes (^{111}Cd and the ^{113}Cd) cannot be found in the spectra from the startup of the reaction, that already did show LENR with about 40% above background. Cadmium lines only did shine up after the full activation of the fuel.

The simplified reaction behind this is:



Whether this reaction runs stepwise $^{107}\text{Ag} + \text{D}^* \rightarrow ^{109}\text{Ag} + \text{D}^* \rightarrow ^{111}\text{Cd} + \text{D}^* \rightarrow ^{113}\text{Cd}$ or as given first has to be investigated in deeper detail.

Also the two/three step reaction $^{107}\text{Ag} + \text{D}^* \rightarrow ^{109}\text{Cd} \rightarrow ^{109}\text{Ag} + \text{D}^* \rightarrow ^{111}\text{Cd}^* (\rightarrow ^{107}\text{Ag} + ^4\text{He})$ is possible * for excited. We call this a Helium spallation reaction path.

Similar things happen also for Samarium/Erbiun. In fact we show such a path for Samarium in all detail in a later chapter. But energetically ^4He spallation only produces net energy starting around Nd. So in the region of the periodic table $^4\text{He}^*$ is added to an isotope as this produces more energy than D^*-D^* fusion alone.

Why do we not prominently see the terminal lines of ^{107}Ag ? A so called "base line is energy" emitted by a gamma state that directly falls back to the ground state. Lines from one magnetic state to another magnetic state, that finally ends in a magnetic base line state obviously can fully "down scale" gamma state/fusion energy, if all involved intermediate states are magnetic states (see example Fig.4). The base state with its associated magnetic moment is able to couple with the magnetic $\text{D}^*-\text{D}^*/\text{H}^*-\text{H}^*$ that is embedded in a grid and can resonantly transfer phonon energy – see also Hagelstein[15]. We could also argue that the base state is blocked by an attached D^*-D^* that lowers its energy below "0". Only if the final phonon down scaling chain is too slow then gammas do occur! Or also in case of ^{155}Gd , when there is a gap between two magnetic states as we e.g. can see in ^{155}Gd for line from 251.7keV to 60.0keV. After 251.7keV all follow up lines are active (Fig.5.b column 3 red marked).

The ^{109}Ag 44.700keV line always shines up with a high relative count to background but with in total a low count. But the 60keV line of ^{155}Gd shows a high activity as it cannot directly couple via a magnetic ground state.

Before we present a small subset of $\text{SO}(4)$ physics that is needed to understand how gamma radiation is produced we will make a short summary.

2.3 Short Overview

What we did show in this introduction part was:

- Mixtures of selected magnetic isotopes, Deuterium loaded, emit gamma radiation some even without any heating/stimulation.
- LENR reactions can directly produce ^4He or add Hydrogen/Deuterium to any Isotope.
- Isotopes with magnetic decay paths can down-scale magnetic fusion excess energy without emitting gamma radiation.
- As spectra do show: Nuclear (LENR) reactions are temperature dependent!
- Such nuclear reactions need a new model to explain why this is possible.
- $\text{SO}(4)$ physics explains the physical structure that is responsible for gamma radiation.

Despite 100 years of modeling and the collective claim of success by current physics - the standard model (SM) – has no clue of real dense matter physics. SM has not the slightest idea which mechanism drives the gamma decay of an excited isotope – produced by cold fusion - and of course even worse SM has no clue about the real particle structure and thus how fusion works.

The full overview of the real particle structure up to ${}^4\text{He}$, ${}^7\text{Li}$ is given in [7]. We here do restrict the explanation of SO(4) physics to the perturbative mass only that is responsible for the energy-holes that can accept a gamma quantum of energy.

3 Short introduction to SO(4) physics

Classic physics (SM) is axiom based and suffers from the missing knowledge about how charge and mass are related. In fact SM – QED/LQCD in respect to dense matter is a historic failure as nobody was able to fill the missing gap. The idea to mathematically project matter to a single abstract field is an obvious violation of the reality – matter generates fields! - as all matter is given by interacting masses/charges that do not have a common fixed point. As the basic proof of computation theory about completeness does show: A model that is based on a closed formalism (group theory operator based formulas must be closed!) is logically not able to model a communicating coupled system. Communicating in the physical reality means: Exchange of energy!

Other long time known failures of SM are the missing integration of a toroidal charge surface to avoid infinities and worst the missing connection to classic Maxwell equations/forces. Internal magnetic fields/energies are not a part of the model. This - the inclusion of magnetism - has first been done by R.Mills GUTCP [16] that is a somewhat more complete model, that also still suffers from most classic modeling limitations.

3.1 What is the base of SO(4) physics (SOP)?

Basically SOP shows how to integrate/project Maxwell equations, basically the forces, into 6D dense matter structures. All mass is classic EM mass and “occurs” between magnetic flux lines and topological charge. All charge is classic virtual (topological) charge generated by nested magnetic flux.

From this it is obvious, given by the nature of magnetic flux, that the surface of the acting physical space must be single sided, because magnetic field lines do not cross. The topology must be toroidal as the finally generated external visible charge cannot have a singularity. SO(4) is the first space that allows us to express Maxwell equivalent force equations under total symmetry in connection with the needed topology (2:1 force action[17]) due to its Clifford torus (CT) center symmetry space. Further it is well known that the CT is a minimal Lagrangian surface[18]. That means the CT is an absolute “center” of mass & force and all deviation from its surface leads to excess energy orbits.

As charge and mass both must be in average time invariant the core formalism of SOP has no direct time dependency. This is a corollary of the fact that charge is not oscillating or a has no wave nature! The nuclear

core structure of stable particles is given by the 6D SO(4) symmetry based magneto static solution of the Maxwell equations. This model thus is 180 degree complementary to what SM(QED, QCD,LQCD) has tried.

3.1.1 How does fusion of matter work?

SOP can give an exact picture of the fusion process. All details for the fusion reactions $e+p \rightarrow n$, $H+H \rightarrow {}^2\text{H}$, ${}^2\text{H}+{}^2\text{H} \rightarrow {}^4\text{He}$ or ${}^2\text{H}+H \rightarrow {}^3\text{He}$ can be given - see[7] - with exact energies and structure change.

The basic physical process that classically is called fusion, in our terminology is called flux compression. Why? The fusion reaction $H+H \rightarrow {}^2\text{H}$ obviously does free space-time energy. As magnetic flux lines cannot disappear and radiation is different from magnetic flux, we must find an explanation how nature generates the freed fusion energy. From mechanics we know that in 3D space a body can have 2 fully independent rotation axes. In SO(4) 6D space 5 independent axes are possible. Each rotation axes of a rigid body can store its own momentum (hence energy). (e.g. 3 rotations inside the same volume can store more energy than 2 rotations = less space time volume is needed!) Thus the fusion process is equivalent to starting one more rotation. In SOP, the amount of energy freed is defined by 3 so called flux compression constants (named 1FC,2FC,3FC), that have an exact physical meaning and basically only depend on the fine structure constant and the golden ratio (3FC).

Because all particles own a nested “wave structure”***** only the outermost waves (= rotating flux lines) can act (emit gamma energy) in the fusion process. One further restriction for fusion is that the acting waves must be equivalent in size and dimension to enable the production of a virtual charge that finally stabilizes the bond.

We describe fusion as a sum of all “wave” interactions that finally show how the resulting fusion energy is produced.

	eV
a) DD bond (n+p+e) delta E	2'224'572.773
b) 2*proton 3D pot = (2*m _p *2FC')	2'179'436.654
c) 2* 4D potential (sec. radius)=(2*m _p *1FC')	40'499.503
d) 4* electron perturbative mass 4*m _{ep}	4732.415
e) Delta before repulsion (a-b-c-d)	-95.798
f) 2*3D pot of 4D pot mass = 2*c*2FC'	94.073
g) 2*4D pot of 4D pot mass = 2*c*1FC'	1.748
delta mass (e+f+g)	0.023

Fig. 6 Deuterium orbit masses

For in depth details look in [7]. In Fig. 6 line a) shows the measured Deuterium fusion energy if a neutron and a proton do join. Line b,c show the amounts of rotation energy that are removed, when the two proton 3D/4D flux lines projected on the two torus radius dimensions each form out a new (1x1)x(1x1) coupled rotation. One rotation is given by the proton-proton coupling the other the by the proton “electron” (charge) coupling. Line d) shows the virtual charge related energy that “is produced” to balance the fused flux. Lines f,g) shows the repulsive energy (given as related to the electroweak and electro strong force constant 1FC', 2FC') generated between c,d and b,c.

$$(m_{ep} := 1183.1037 \text{ eV} = (m_e * (1 - 1/e_g^2)) - e_g \text{ is the electron g-factor})$$

***** We here uphold the wave picture as it allows a smooth integration (explanation) with the dissipative part.

What we not show in Fig 6. is that a neutron also holds one m_{ep} mass and in fact this is what causes a perturbative (excess energy) orbit.

If the flux of two protons starts a new shared rotation then the resulting body needs less space to store the same amount of energy. All mass flux runs on or along the Clifford torus (CT) center symmetry structure of SO(4). The on torus flux is given by the 4 rotation SU(2)X(SU(2) coupling of dense mass, where as the excess mass flows along the CT surface and does 3 rotations. In the proton (and Deuterium) case the 3 rotation excess mass also defines the magnetic moment.

In the deuterium case only excess mass does fuse which is classically equivalent to an electro strong fusion reaction. (There is no strong force action in the Deuterium nucleus!!) This also explains why Deuterium has no gamma structure. The 3 p-p bond rotations (Fig.6 line b) do each manifest in a 2179.436/3 keV wave weight of about 726.5keV. (727.2keV for a 1/3 p-n bond using the neutron weight). The ¹⁵⁵Gd state of 729.6keV closely reflects this energy together with half the coupled charge mass of 2.36keV. In fact many isotopes show very simple relation with basic SOP wave energies.

One general “problem” is, that the SO(4) approach potentially has more than 1 degree of freedom. E.g. in the n/p case, if two mixed 4,3 rotation particles (e.g. 2 protons) join then the “fusing part” of the 3 rotation mass, when adding one more rotation, joins the 4 rotation mass. If a photon meets a proton orbit then the two rotation photon ads one rotation and temporarily joins the 3 rotation proton flux. So effectively fusion “photon resorption/absorption” always first is handled by the lowest involved rotation masses. The same we do in Fig.6. We also can exactly do the same with p+n instead of using the basic building structure from e,p. This is the final reason why we most of the time, at least, can give two different projections to basic particles for any fusion process. One is the view from the joining masses the other from the resulting mass once using particles (n-p) or using basic p-e-p bonds.

The space freed (e.g. Fig.6 a), classically is a small volume, that once has been filled with space-time energy. If we start from particles (p+n) this is equivalent to “generate” a flux hole and because this hole is also depending on the tighter structure it must be compressed too. These two facts are important for the calculation of certain gamma energies.

Summary:

Protons as we show in [7] “on the surface” form out 3 rotation axes where classically each axis corresponds to a wave. The compressed (relative to 2 rotation photons) flux with 3 energy eigenvalues is also called 3D/4D flux because the associated mass does 3 rotations (3 orthogonal rotation planes) in 4 independent dimensions. Thus in Deuterium we see 3/3 of free p-p 3D/4D flux

waves. The toroidally symmetric charge mass binding structure of Deuterium has recently been confirmed by neutron measurements[19].

Deuterium does not own a gamma spectrum because there is no containing/stabilizing structure, that holds either the proton or the neutron together. The first nucleus with a gamma spectrum is ⁶Li. ⁴He has no gamma spectrum too, because it owns no 3D/4D excess mass waves. ⁴He only emits a gamma ray in a decay reaction.

3.2 The ⁶Li model and its first two gamma lines

There is a quick solution to model the basic SO(4) wave structure of all isotopes based on the fact that in average always a neutron and a proton do bind. With a simple progressive division you can determine the so called SOP 4D quanta and the number of free 3D/4D flux waves for all known isotopes. This has already been shown about 4 years ago in NPP version 2.1. The detailed wave model for ⁶Li looks as following: See Fig. 7a. ⁶Li can be modeled by a ⁴He nucleus with two (1/3) p-p wave connection to a ²H nucleus. Why only 1/3 waves between p and the alpha particle? The alpha core already does 4 rotation and thus only one binding is possible. So the total free 3D/4D flux is 5/3 p-p wave couplings.

The mass delta of the sum ⁴He+ ²H – ⁶Li is shown in Fig. 7a line g). Fig. 7a line h) shows the standard SOP basic radial flux compression constant for one dimension (= 1FC*2FC*3FC) and c) is the charge related compression when charge moves from a torus 9/8 excess energy form factor to an 8/8 CT symmetric form factor - circular orbit. j) shows 2/3 of a deuterium (1x1)X(1x1) two radius bond. in ⁴He all flux orbits have a (2x2)X(2x2) structure and only a matching pair can attach. The proton has a (3x2) structure which implies that the 2:2 can go into resonance.

In general a p-e-p “bond” can do 5 “connections” as the virtual neutron structure offers two additional energy holes. This 2/3 bonds are attached to the 4 rotation mass of ⁴He. As we did show in [7] the bound 3D/4D flux in ⁴He undergoes further compression than seen inside a proton.

a) m_{ep}	1'183.104
b) $m_{ep} \text{ rot} 1/9$	131.4559670958
c) electron photonic mass rel. $((m_e - b)/m_e)$	0.9997427471
d) ⁶ Li mass	5'603'050'886.4772
e) ² H mass	1'876'123'913.2785
f) ⁴ He mass	3'728'401'292.0028
g) delta mass = (e+f-d)	1'474'318.8041
h) 1D pert	0.9959335244
i) 2/3 2FC'+1FC' proton wave	1'479'957.4379
k) 1D compression/charge 1/9 = (i*h/c)	1'474'318.4999
Rest error absolute (g-k)	0.3043

Fig. 7a ⁶Li structure

Fig. 7 line k) shows the by radial strong force (h) “compressed” and by (c - charge) expanded mass. The virtual charge that binds the Deuterium an alpha particle does not follow a circle orbit.

a) Proton relativistic radius	0.8376530074
b) 6Li radius (russian data!!) in fm	2.5432
c) 4He radius = 2*a	1.6753060148
d) delta = b -c (eff Radius = 1/2 of diff.)	0.8678939852
e) μ 6Li in Magneton units	0.8220566700
f) Nuclear magneton	0.5050783699
g) effective μ 6Li moment = e*f	0.4152030428
h) calc. moment 2 off 5 waves (2/5)*ec*d/4	0.4168672445
i) relative match	0.9960078377
k) 1D force = 3FC*2FC*1FC	0.9959335244
l) 1D flux compression = k/j	0.9999253889

Fig. 7b ⁶Li magnetic moment

In general in SOP all atomic mass calculations are shown as sum of the energy holes left behind/produced by various p-p or p-e-p bonds together with their coupling. Thus we explain fusion by the different orbits doing mass/flux compression/expansion

In SOP all energy is EM energy. Unperturbed magnetic flux can be modeled as bound EM (magnetic) flux lines exactly following a curved 6D manifold with no added virtual energy (energy/mass flows in direction of the magnetic flux line). Orbits following the CT are circular and carry no mechanical (l=1) excess energy! All other excess energy rotations generate a mechanical rigid mass/moment that couples orthogonal to the manifold. This added virtual mass is mechanically stored by amounts of rigid torus form factors being $l = 9/8$ or $7/4$.

The basic force factor (3FC*2FC*1FC) we do find in all particle models of SOP including the proton magnetic moment. SOP force factors act symmetrically either these do compress flux (going to CT conform circular 4 rotations) or expand flux (going to flat torus 3 rotations). In the proton case (magnetic moment, mass) the flux is expanded. In the ⁴He (4 rotations CT conform) case flux is compressed (toward most dense orbit) – in the free 5th rotation dimension. Here as the charge used to bind ⁴He - ²H stays in the proton frame too its mass is expanded.

The changes in the compression (5639eV) of the internal 6Li orbits seen in Fig.7 a lines j,k are exactly confirmed by the gamma spectrum see 3.2.1 below.

Summary ⁶Li: The two protons of deuterium that “orbit” ⁴He alpha particle kernel start each a one (of 3) wave rotation with the ⁴He 4 rotation core. These two waves stick to ⁴He and thus are compressed by the standard 1D force factor Fig.7 line h red. The coupling charge with the Deuterium over the induced virtual charge Fig. 7a. line a changes from 8/8 CT conform to flat torus to 9/8.

We can also do a quick approximation of the ⁶Li magnetic moment M by using the standard formula. But nuclear charge radius data is very low grade! The magnetic moment is given by.

$$M_{Li} = e * c * r_m / 2; \text{ or with acting mass factor } M = m' * e * c * r_m / 2.$$

The only free flux is the 2/3 waves so the acting mass is 2/5 of the ⁶Li 3D/4D flux. Thus m' is 2/5. The torus diameter. see Fig.8. is the difference between the ⁶Li radius (Fig. 7b ,b) and the ⁴He charge radius that is double the proton

relativistic radius (Fig. 7b ,a). (Fig. 7b ,h) show the formula for the unadjusted moment. As we see in the mass model and gamma lines below too the compression works in the moment for 1D and the corrected moment (Fig. 7b line j) is 4 digits exact as the radius.

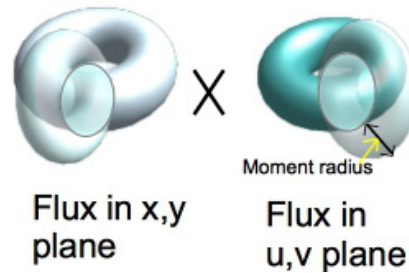


Fig.8 ⁶Li coupling orbit projection

3.2.1 The first two ⁶Li gamma lines (states)

The first 6Li gamma line Fig. 9a can be modeled as the break up of the internal “deuterium” p-p bond. The second line, Fig. 9b, is an inner excitation of the ⁴He – ²H (⁶Li) bond. Just to repeat once more: The flux that interacts with gamma radiation is the 3D/4D compressed excess mass (its energy holes) that runs along the CT doing 3 rotations at once. Thus the 3D/4D excess mass naturally splits in three “waves” each corresponding to one independent rotation.

Gamma excitations are defined by the number of acting waves and the harmonics of the excitation. Here in ⁶Li we in total do have 5 waves of in total 5/3 of a proton-proton bond that can act. Inner (coupled) excitations, as seen in the second line, usually are based on integer fractions (x/5) of the (5) involved waves. In ⁶Li two waves are bound to the ⁴He core and 3 waves form the classic deuterium bond. Thus any of these 5 waves can split by 1/5. But for a standard SO(4) coupling two such 1/5 waves quantities must occur in parallel. Here the only allowed (see also 3.3.2) simple eigenvalue split (of 5 waves) in 3 dimensions is 1:3:1 as the coupling waves have different weights than the p-p bond waves. The excitation of the ⁶Li second gamma line is a higher harmonics (of 1 → 2 → 4) of the 2 binding 1/3 waves, leading to a 4:3:4. mass ratio coupling (see also below Fig.10)

6-Li first line	2'186'200.0000
a) 2*proton 3D pot = 2*(m _p *2FC')	2'179'436.6538
b) m _{ep}	1'183.1037
c) virtual mass = b) *1/9	131.4560
d) charge rel. compression. ((m _e -c)/m _e)	0.9997427471
e) Flux compression 6Li in fig.7a (j-k)	5'638.9380
f) Flux expansion a/d ²	2'180'558.4195
Total line energy e+f	2'186'197.3575

Fig.9 a) ⁶Li first gamma line

Fig. 9 a. The deuterium bond split, in a first approximation, is given by the proton-proton bond energy shown in Fig. 9a. line a); (also in Fig 6a .b)). Fig. 9a line e) shows the same value we calculated in Fig.7a lines (j-k). A photon has a (1x1) – 2 rotation structure.

a) second line	3'562'880.0000
b) Mills gamma $\gamma^* = I/(1+\pi a^2)$	0.9998327339
c) acting mass reduction = b*a	3'562'284.0510
d) Flux compression 6Li in eV	5'638.9380
e) 2*proton 3D pot ($m_p * 2FC' + 1FC'$)	2'219'936.1568
f) 2/5 4 fold coupling = (2/5)*e*4	3'550'984.1148
g) = c -2*d -f error in calculation	22.0601

Fig.9 b) ⁶Li second gamma line

When the gamma energy is added then obviously the binding bond compression is reversed as now the added gamma energy is an excess mass. Further new binding charge is generated for the added gamma energy and the “orbiting” ²H. Thus the compression factor Fig. 9a line d) must be applied twice – once for each photon rotation. As a result of photon absorption the ⁴He – ²H (⁶Li) bond compression is reversed. Fig.9a line e) = Fig 7a. value lines (j-k).

For the inner excitation Fig. 9b we must still use the old general approach. The conversion of a photon 2D/3D mass to 3D/4D flux mass is given by the so called Mills gamma**** and leads to as somewhat lower acting mass Fig. 9b c). In this case we exactly know how much energy is needed to uncouple the waves Fig.9b line d) – same as Fig. 9a e). Such a calculation is only possible for cases where we know the exact wave structure. In a general case we currently must use an approximation for calculating the activation energy of an energy hole. What we also can see, is that due to the inner excitation the bond between the ⁴He core and the p-p orbit loses a part of the coupling force and hence the compression reverses Fig.9b line g factor 2*d. In the first line just the compression vanishes. We could also say that due to the added photon mass the wave weight doubles 2 times and thus binding energy must increase accordingly.

****Mills gamma $\gamma^* = 1/(1+\pi a^2)$ compensates for the overall change in the De-Broglie radius potential when 2 rotation mass is added to 3 rotation mass. This small mass fraction is stored globally and upon release of the gamma quantum is added again.

The first line involves a local structure only! In the second gamma line case the full ⁶Li mass is still regularly connected, where as in the first line case an internal structure is broken and the action is no longer symmetric. Mills gamma so far has been working very reliably as you will note in section 3.3.2. It seems to reflect the metric change for mass weights at different (2,3) rotations. Thanks to this we can use a 2 rotation photon mass and use it as a 3 rotation equivalent.

3.2.2 Physical shape of gamma excess energy

Gamma energy can only be added to a nucleus with a stable 4 rotation kernel structure. Gamma energy always fills existing energy holes (of the so called 3D/4D mass structure), that were left behind by the mass compression of basic particles to dense mass nucleus structures. Gamma energy most of the time is temporal excess mass and thus, basically must be modeled by classic (3D,t) physics. 3 rotations in 4D are a perfect cover of S³ and all Eigenvalues are independent in 3 out of 4 D and thus do

not radiate.

⁴He is an exception as it contains a stable 4 rotations kernel mass but no free 3D/4D flux. Thus the only possibility to add a gamma quantum to ⁴He is to crack the 4 rotation structure, which implicitly violates the above rule, as demonstrated in the follow up decay of ⁴He into the possible substructures (D,T,³He,p,n).

If an energy hole gets filled (by gamma energy) then the balance for one rotation is lost and the three rotation mass now stays in 3D,t only.

Below the solution matrix for the momenta of inertia for all three classic dimension of a force-free coupled 3D rigid 2D symmetric mass system is given. As EM mass is always flowing inside a torus volume (with 2 identical radius) two of the three orthogonal rotation axes have the same inherent moment of inertia.

$$M = \begin{pmatrix} \frac{1}{\Theta_1} & 0 & -\frac{\cos \vartheta}{\Theta_1} \\ 0 & \frac{\sin^2 \vartheta}{\Theta_1} & 0 \\ -\frac{\cos \vartheta}{\Theta_1} & 0 & \frac{\sin^2 \vartheta}{\Theta_3} + \frac{\cos^2 \vartheta}{\Theta_1} \end{pmatrix}$$

Fig. 10 From [24] . The moment (M) of inertia Matrix

The trivial solution of Fig. 10 can be found by setting $\cos(x) = 0$ (and implicit $\sin(x)^2$ will be 1!), what leads to the following final relation for the energy Eigenvalues: 1:1:M1/M3 (or M3:M3:M1) where the numbering of the dimensions is not important because of the “ring symmetry”. This, in general (in 4 independent dimensions) leads to the following two possible symmetric energy (proportional to momenta of inertia) distributions: 1:y:1 or x:1:x. As a conclusion of this, we see that the free flux always occurs in quanta of 1/3 (there are always three rotators = waves and 1:1:1 is always a solution). Any symmetric addition of a 1/3 excess quanta leads to a stable simple 3D/4D rotator! One more important thing we must note is that any natural number of waves leads to a symmetric rotator of the above form. This is important as we must guarantee a seamless quantization of the rigid rotating mass!

The above Fig. 10 solution just works for simple 3D/4D mass flux holes with no complex 4D coupling. If we add one more dimension (a “center” 4D coupling) to the Fig. 10 tensor then we get a higher order tensor with 4 x 3 x3 dimensions. That way it is possible to analyze complete gamma spectra of isotopes. About 70% of all gamma lines can be found by this approach. Other lines e.g. are based on neutron energy holes charge coupling changes as seen e.g. in ⁶¹Ni[20]. There are also other, different solutions for the Fig. 10 system that are responsible for ultra fast (short time stable excitation lines).

3.3 Possible sources of gamma lines

Above, in the case of ⁶Li we already could show two basic

sources for gamma lines. Most Isotopes do host some excess proton, neutron, Deuterium and “charge mass” structures, that form out various bonds. So one gamma radiation source is a cracked p-p or e-p bond. A more subtle source is a 3 rotator 1:x:1 or x:1:x or more general n:x:n x:n:x excitation. Even simpler gamma sources stem from refilling an energy hole of an internal, bond.

Higher order 4D coupling leads to a complex splitting of the lines given by the 3D/4D mass to 4D mass relation.

See sample below

3.3.1 ¹¹⁷Sn the island of stability

Sn is an extraordinary set of isotopes. It covers a large range of SOP orbital quantum number from 47 to 55 4D quanta released. ¹¹⁷Sn itself in total has 51 4D quanta released, which leads to a special orbit structure of (7,7); (7,7);(7,7); (7,2);(0,0);0,0). It owns a long living (> 1 week!!) gamma state at 314.58keV. This state has the exact weight of two coupled neutron waves and does express a magnetic moment. In our analysis, given in Fig. 11 many gamma lines match multiple times at various primes/fractions. The red marked fields show the best matchings with at least 5 digits precision relative to line energy. The blue matches usually are lower grade, but still > three digits matches.

Sn117	1 x 7	1 x 7	1 x 7	2 x 7	2 x 7	2 x 7	2 x 7	2 x 7
Final lines keV	13/49 5/21	20/49 5/6	29/49 3/5	7/49 1/3	6/49 4/3	13/49 5/6	24/49 6/7	43/49 1/3
158.562	0.092051	0.017940	0.017408	1.000474	-0.171169	-0.175421	-0.109274	-0.174201
314.58	1.000117	0.199061	0.198626	2.327705	0.040955	0.041349	0.025151	0.038445
1004.53	5.015806	1.000025	1.000016	8.197049	0.979019	0.999956	0.619610	0.978816
1019.92	5.105380	1.017892	1.017892	8.327971	0.999943	1.021339	0.632870	0.999792
1179.7	6.035341	1.203381	1.203480	9.687205	1.217182	1.243335	0.770536	1.217565
1446.2	7.586441	1.512761	1.513025	11.954237	1.579518	1.613606	1.000152	1.580793
1468.6	7.716815	1.538765	1.539043	12.144852	1.609974	1.644729	1.019452	1.611323
1510.1	7.958355	1.586943	1.587246	12.497889	1.666397	1.702388	1.055208	1.667895
1578.25	8.355006	1.666058	1.666404	13.077635	1.759055	1.797075	1.113926	1.760771
2048.2	11.090238	2.211624	2.212260	17.075458	2.398004	2.450017	1.518834	2.401292
2128.6	11.558187	2.304960	2.305646	17.759414	2.507317	2.561724	1.588106	2.510873
2280.4	12.441703	2.481185	2.481965	19.050763	2.713706	2.772633	1.718897	2.717770
2304.6	12.582553	2.509279	2.510073	19.256630	2.746608	2.806256	1.739747	2.750754
2367.3	12.947483	2.582068	2.582901	19.790014	2.831856	2.893371	1.793770	2.836211
2415.9	13.230348	2.638487	2.639351	20.203450	2.897933	2.960895	1.835643	2.902450
2515.8	13.811792	2.754462	2.755386	21.053290	3.033758	3.099695	1.921717	3.038610
2590.2	14.244820	2.840833	2.841803	21.686204	3.134913	3.203065	1.985820	3.140014

possible quantization steps) base line splits.

The basis for the analysis shown in Fig.11 is a 4 rotation Lagrangian that approximates the 4 rotation coupling with the basic 3 rotation coupling (first shown in [21]). All line energies given in the first column are so called base lines. This are gamma lines, that directly fall back to the “0” energy level. Line 1 (fig.11) shows the 4D coupling weight that either is 7 or 14 4D quanta. Basically every involved line can split into any prime factor rational quantity.

The fields in red shows the line energy(column 1) that exactly matches the given excitation pattern

So in the, as expected, best matching column 5 the (7,7) strong force quanta (in total 14) couple with 1/7 of its weight to the 1/3 wave of the primary acting 3D/4D flux formed by p-p bonds. This is the most simple possible 4D coupling.

Column 5 shows that 5 additional lines just are higher (integer multiple, usually primes or simple prime factors) excitations of the basic line.

Keep in mind that ¹¹⁷Sn has an exceptionally highly

symmetric structure regarding the strong force coupling, Its a rare exception to find 5 simply connected (Fig.11 red/ green) lines with the same simple coupling relation. Further the 2515.8, 1578.25, 1446.2keV lines can also directly fall back to the connected 158.562keV state which gives high evidence that the model is showing physical facts.

Each computed column in Fig. 11 is based on the same matching parameters just the line energy varies according column 1. What we also quite often see is that two different pairs of weight factors can delivers almost the same result. Compare column 6,9 or 2,3.

3.4 Summary

SOP allows us to model the internal structure of isotopes and to find the acting waves, based on energy holes, that form a gamma state. We here just wanted to show that the connection between gamma states is complex, but often can be explained. As we in the following will have to analyze spectra with > 300 active lines of stable isotopes, we must know how the internal transport of gamma energy works. The impressive picture given in Fig.11 column 5 shows that some gamma lines are internally connected and are just “higher harmonics” of a magnetic base line. So this early theoretical work from October 2017, confirmed by published data [10] did later help to understand why the ¹⁵⁵Gd 60keV was over-represented in relation to preceding lines.

In the following we will treat the effect of internal downscaling of gamma energy.

4 How down-scaling works

As per definition cold fusion or LENR describes the fusion process of elements without providing kinetic input energy. All classic fusion processes use high kinetic input energy or exploit (in case of fission) internal isotopes instability. As in LENR we have no resulting momentum, we cannot transport fusion energy by kinetic energy unless we produce unstable nuclei.

Thus in cold fusion energy can only be transported by exchanging magnetic flux. According to Faraday’s law changing magnetic flux can induce charge, which leads to EM coupling or magnetic polarization.

4.1 Origin of magnetic flux

A pair of dense Deuterium (Fig. 12 D*-D*) effectively is a strong perturbed magnetic mass that oscillates in 4 (2x2 coupled) rotation dimensions. In SO(4) physics we show that two protons can join their 3D/4D flux waves and start a common new rotation. This 3+1 rotation state finally wants to relax to a symmetric 2x2 (4 rotation) “wave” structure. In a three D projection we can indicate this as a torus that gets squeezed and afterwards expands again. The magnetic polarization has always the same vector but the field strength is maximal in the wide stretched situation. This is explained by SO(4) physics [2] that shows

that Q^2 (Q for internal binding charge) is proportional to the product of “mass-flux” * radius. Such a field can be as high as 10^{13} Tesla.

Magnetic isotopes work like antennas, that are able to synchronize with the oscillating D^*-D^* field.

SO(4) physics shows that gamma states are produced by so called energy-holes of the joined 3D/4D flux. These holes e.g. the ^{61}Ni 67.418keV state, can be re-filled and the nucleus transforms to a transient, classically excited state. Normally this magnetic binding gets extended to shell electrons and finally a chain of coupling magnetic states shines up that spin aligns all the acting fusion elements. These chains allow for a steady flux of magnetic energy until D^*-D^* becomes ^4He at rest. Nickel allows a high degree of magnetic polarization, which we exploit in all kind of magnets.

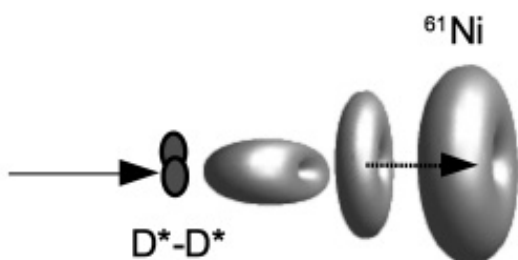
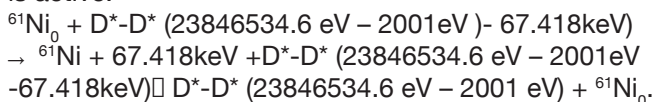


Fig.12 Deuterium Nickel coupling

To be able to transport magnetic energy the accepting gamma orbit must be in a harmonic relation with the excess flux that will be released during the fusion process. This process is symmetric as long as no phonon coupling is active.



But the D^*-D^* frequency is much higher (energy state live time much shorter) than the live time of the ^{61}Ni 67.418keV state that has a pretty long live time of 5.34ns. So the chance that ^{61}Ni can send back the energy to D^*-D^* is very low. But also the chance to see a ^{61}Ni gamma ray is low as the ^{61}Ni gamma state is always coupled to D^*-D^* , which means its energy does not match the free gamma state level. What our measurements imply is that at most 10^{-8} of all LENR reactions lead to a gamma quantum emission. This most likely is possible when a fusion reaction delivers no more energy to the gamma state and the final phonon coupling abruptly breaks.

Nickel can very efficiently connect to Hydrogen. So if Nickel is connected to a cluster of H^*-H^* or D^*-D^* then it can transport the 67.418keV to about 34 D^*-D^* what makes them ordinary D again. It can also couple to a broad, harmonically coupled, correlated phonon state, see Hagelstein[15]. Key is, that lower energy states must act much faster, than the refill state of the higher energy state. This is usually the case with phonons.

For oscillating D^*-D^* we have no experimental data for the exact range of the real field strength and its oscillation frequency.

An even more important feature of some magnetic decays is the fact that the base state (0 keV) can have a different magnetic momentum polarity than preceding excited

states. This leads to an extreme change in field strength, which induces charge that can act in multiple ways. E.g. by direct emission of radiation or modulating inner orbit electrons that later emit X-rays.

So the basic hierarchy of energy transport is fast \rightarrow slow \rightarrow fast state. What is equivalent to: Fusion \rightarrow Nuclear state \rightarrow orbital or phonon states. The longer the lifetime of the nuclear(gamma-) intermediate state is, the fewer low energy partners are needed to accept the state energy.

Talking classically in so called layers of reference frames we have 4 rotation (fusion-) energy that must be disposed. The first step is 3 rotation energy of a gamma state. Then classic electron shell energy with two rotations (or gamma photons) is the first possible final step. So we at least traverse 2 reference frame steps. If we look at phonons as one dimensional excitations (modeled as spring coupling), then we pass three reference frames. If we assume that one difference in reference frames is given by the inverse of $\alpha/2\pi = 861 (= 1/2FC)$, the SO(4) electro strong coupling constant) then the middle state (for $D-D \rightarrow ^4\text{He}$) synchronizes with a magnitude of 27'696eV and the lower state with 32eV and phonons in the range of 0.04eV. This is just given to show the magnitudes of possible coupling states we encounter in cold fusion.

Swartz [22] did report an other possible, even much lower energy coupling as he measured the Deuterium fine-structure coupling frequency in his NANOR process. This energy transfer needs no secondary coupling at all as here energy directly is emitted as an EM wave. One quantum here, in den ^2H case, is $1.35 \cdot 10^{-6}$ eV.

4.2 Summary of down-scaling

Various experiments do show that the excess energy produced by cold fusion reactions is transported by different forms of magnetic flux. Large amounts of fusion energy can only be transported by large quanta of so called magnetic gamma states, that is by isotopes that own more than one connected magnetic state. This works best if the ground states expresses a magnetic moment too as shown for Silver. Even better is when the ground state and the decaying state do express a different magnetic polarity. This decay path has also been shown by [15] for ^{57}Fe based starting with ^{57}Co . ^{57}Fe is one isotope that thanks to this feature is helpful for LENR.

A slower downscaling-transport mode is possible by relaxed D^*-D^* states that upon receiving energy become D-D again. But this potentially drains out the proliferation of active fuel for coming reactions.

5 The true nucleosynthesis

Since about 10 years ago Leif Holmlid[3][4][12] performed breakthrough physics that helps us to explain some basic steps of nucleosynthesis. His experiments do show that one can crack a proton with optical ‘photon level’ input energy[3][4]. As all condensed mass behaves as magnetic flux only, one can, with the mediation of a catalyst - induce the formation of clusters of dense Hydrogen (H^*

or D*). As we already did explain, the H*-H* bond release about 500eV. These H*/D* clusters are pure spin matter and look like superconductors. Spin matter alone cannot fuse as the adjacent quantum states do not have the same weight. Only flux of same shape and weight can go into resonance. If one now adds energy to the spin orbits, then the lower quantum state weight is increased and it can go into resonance with next higher state. As photons are always adsorbed and re-emitted these temporarily add “mass” to the orbit. This finally leads to a kind of chain reactions when the combined fusion energy is greater than the proton break-off resonance energy. In [12] ⁴He is one product of the D* cluster reaction but also ³He has been seen, but no ³H. As the reaction runs more or less the same independently of the form of Hydrogen (H/D) and only one end product (⁴He) can deliver the proton break off energy we can assume that the Holmlid reaction works as following:



There is no direct way to produce ²H from two ¹H. Only H*-H* is a possible stable end product. The true first step in nucleosynthesis thereof is $4 \text{ } ^1\text{H} \rightarrow \text{}^4\text{He}$. The energy of such a H* cluster reaction (e.g. $9 \text{ } ^1\text{H} \rightarrow 2 \text{ } ^4\text{He} + \text{K}^+, \text{K}^0$) is high enough to crack a proton[4], which leads to a Kaon, Pion, Muon particle chain. So basically, as a result of such a cluster fusion, any structure beyond ⁴He can be produced by follow up e.g. muonic fusion reactions. If the result of the cluster fusion is ¹²C then remaining excess energy can produce neutrons, ²H and ³He.

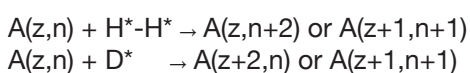
What you will learn here is that the classic standard model ideas about how “nature” produces elements are based on speculative logic only. LENR experiments show that no super novae is needed to produce higher Z elements. The biggest historic error was the claim that ⁴He contains neutrons. Also for higher A, Z isotopes many have claimed neutrons. In reality neutrons are transformed to charge only and integrated into the Alpha wave structure. In fact most isotopes contain only a few “real” neutron structures as the core is formed by conjugated neutron less alpha particles.

5.1 Higher Z nucleus syntheses

As our cold fusion experiments do show, potentially all elements of the periodic table can be produced by the basic reaction of adding H*-H* or D*-D* or H*/D* to a nucleus.

The D* fusion reaction – we measured - following the addition of D* do produce different element chains than the well known Nickel reactions with adding H*-H*. H*-H* can add like a di-neutron or neutron/proton pair. D*-D* or just one D* can add as two protons or a neutron/proton combination. This allows for direct horizontal or vertical progress in the periodic table of elements (isotopes).

So the basic rules are as following::



The $A(z,n) + \text{H}^*-\text{H}^* \rightarrow A(z,n+2)$ reaction type is well known and proven for Nickel. Here the reaction dominantly runs from $^{58}\text{Ni} + \text{H}^*-\text{H}^* \rightarrow ^{60}\text{Ni} + \text{H}^*-\text{H}^* \rightarrow ^{62}\text{Ni} + \text{H}^*-\text{H}^* \rightarrow ^{64}\text{Ni}$ that has been shown in a recent element/isotopes analysis. As SOP modeling did show, Nickel owns excess charge mass(es) which compensates for the missing “neutron charge”.

The $A(z,n) + \text{D}^* \rightarrow A(z+2,n+2)$ or $A(z+1,n+1)$ reactions can also deliver a final $A(z,n+2)$ state when the intermediate state(s) are unstable and do beta⁺ decay.

There is a second type of cold fusion reactions that is known as disproportion reactions.

Basically in the reaction $2 A(z,n) \rightarrow A(z-1,n-1) A(z+1,n+1)$ a deuterium substructure is exchanged. Also single nucleon exchange has been seen in the lithium case. $2 \text{ } ^7\text{Li} \rightarrow 2 \text{ } ^4\text{He} + \text{ } ^6\text{Li}$. This path has been measured by Lipinski’s [23]. But in the universe hydrogen is the dominant mass and disproportion reactions definitely need a background of a stable star like earth’s sol.

5.2 What we in detail will show

We will show the progress in the nuclear chain (evolving isotopes) by looking at gamma spectra from LENR reactions.

In the following we first will look at the Pd → Sn cycle and then at a large chunk of the Ce → Ho cycle. There are some more, but smaller cycles we will not treat here.

The results we here do present are based on Deuterium adding reactions. But even 99.8% pure deuterium contains a large fraction of protonic Hydrogen, that can activate some side paths what potentially can disturb the picture. We also, so far, have no experimental evidence that mixed H*-D* pairs are allowed or do exist.

There are some limitations regarding gamma lines one can see from a powder mixture. Usually lines above 500keV start strong scattering, that gets even stronger for higher energies. So we have no really strong signals above 500keV with a few exceptions, where the background is low. Above 700keV there is almost no usable signal with a few counts being in the range of 6..10 . We also did not extend the calibration beyond the ¹³⁷Cs line. So, due to scattering, some decay cascades for gamma states present holes. It is also difficult to account for the overall scattering contribution to lower energy signals. If you look at Fig.1 then you notice that the excess energy distribution, in general, shows no exponential substructures. Backscattering peaks also would be much broader.

Nevertheless we must note that nobody so far did measure – not even close – spectra from symmetric excitations, we here do see from cold fusion reactions. So we must be aware that this is just the beginning of “new physics” and we here still walk on old ground (tabulated data) we must trust, but don’t know whether it, at the end, really fits.

Lines we mention are visible in at least two different spectra high above background. If there are few occurrences we often label it with T which means: Visible at certain temperature. E.g. HT means at higher temperature only. Furthermore some few lines of isotope X could overlap with isotope Y , then we mention “Y” in brackets. The

only mean to verify a lines existence is to look at the full cascade. This is sometimes difficult for fully magnetic (internal) decays that have one magnitude less counts. The highest complexity we encountered in the analysis of the full Q factor decay of ¹⁵²Sm. A full Q factor decay can trigger a very broad response. So we could assign > 100 lines to ¹⁵²Sm!

As our experiments did show, LENR reactions can be strongly temperature dependent as the downscaling of fusion excess energy finally depends on the terminal coupling with a matching phonon state. So some of the lines we track below are spread over different spectra and temperatures where these are significantly elevated. We most of the time only show the most active single path. For a complete picture one should write more deep exploring software that integrates over all possible decay paths.

5.2.1 Intermediate states

Most intermediate states (e.g. ¹⁰⁶Ag, ¹¹²In) are short lived and some only show up later in the experiment as e.g. we did not add cadmium to our powders. So cadmium (and e.g. ¹¹¹Cd, ¹¹³Cd, ¹¹³In, ¹¹³Sn) lines are a followup product of our reaction and thus the most direct prove for the progress in higher Z isotope production.

We here can just report what we measured. The typical induced Q factor of adding H*-H* or D* - above A=140 is around 11MeV (9..13MeV) for the stable end product. Around A = 100..120 its > 13 MeV. But all intermediates follow different rules and many have magnetic states too. Some also (e.g. ¹⁰⁶Ag) have a choice of two targets for a decay! For the Pd → Sn cycle we did not see full spectral responses that one could expect from adding 13MeV. But around Sm,Gd things look much different. If in a reaction chain like ¹⁴⁸Sm + ²H → ¹⁵⁰Sm + ²H → ¹⁵²Eu → ¹⁵²Sm the combined Q factor is below the ⁴He formation energy, then often it looks like the seen Q factor is the difference between the ⁴He formation and the chain Q-factor. Most likely because D*-D* → ⁴He is downscaled over the magnetic decay path. Here we have no strict explanation. An other big unknown is introduced by the fact that classic gamma spectra often have been measured as a follow up of a kinetic impact. We expect that in a momentum free excitation some decays are forbidden and more magnetic states, than we currently know, do form out. Also the states live time could look totally different if a nucleus is at rest. But this is speculation and needs further cold fusion research!

During some other experiments we did see shifts of entire spectrum parts by 2 or 6keV. This could imply that D*-D* did couple in a way that did allow adding the formation D*-D* binding energy to the gamma state. Such an effect in principle could also spoil the data we here did use. But usually such effects did happen before a full activation and had a short time nature.

5.3 How we match lines

A line exists if it has a predecessor. So we in general show cascading lines. Only in few cases we show isolated lines.

This happens in cases where most decay energies are > 500keV. For lines above 500keV we often look at the center and two neighbor buckets and do the same for the two backgrounds. Lines should be at least 5 counts above background or 50% above background. Even if we are 100% above background is must be at least 4 counts in 2 spectra.

5.4 The Pd → Sn Complex

We here see two possible reaction chains. On chains follows the odd A's the other the even ones. Interesting is to note that most dominant lines we have seen (Fig.3) stem from odd A's. nevertheless we also can see the even mass number isotopes. Starting with tin and after tin (¹¹²Sn) doing follow ups is more or less impossible because most lines are above 500keV, which rarely results in a bucket hit before scattering.

What our measurements show is that just by adding deuterium all elements in this production chain are produced. We do not believe that the measured radiation rate has any strongly defining relation to the true production rate. As indicated, we here can only see whether spectral energies are present or not. The more multiple connected gamma states (a cascade) we can see e.g. for ¹¹⁰Ag, the more reliable the finding is.

Because the Cadmium lines do show up 4-5 x stronger later in the experiment we can be absolute sure that the whole chain did run up to tin.

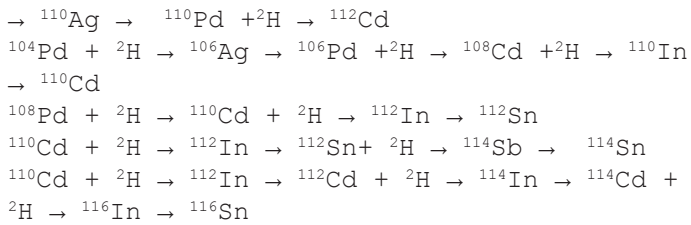
3000n 10.30 M	3060n 30.0 M	1100n 4.11 E	1110n 35.3 M	1120n STABLE 0.87%	1130n 115.00 D	1140n STABLE 0.66%	1150n STABLE 0.26%
< 100.00%	< 100.00%	< 100.00%	< 100.00%		< 100.00%		
1070n 32.4 M	1080n 55.0 M	1090n 4.167 M	1100n 4.0 H	1110n 2.8047 D	1120n 14.97 M	1130n STABLE 4.23%	1140n 71.0 E
< 100.00%	< 100.00%	< 100.00%	< 100.00%	< 100.00%	< 50.00%	< 44.00%	β- 99.50%
1080n 47.48+17 Y	1070n 6.80 M	1080n >1.0E+18 Y	1090n 9.88%	1100n 483.4 D	1110n STABLE 12.48%	1120n STABLE 74.1%	1130n 7.70+18 Y
1.3%	< 100.00%	2%	< 100.00%				β- 100.00%
1050n 41.20 D	1060n 23.80 M	1070n STABLE 31.00%	1080n 2.37 M	1090n STABLE 48.94%	1100n 24.0 E	1110n 7.45 D	1120n 8.130 M
< 100.00%	< 99.90%		β- 97.00%		β- 99.70%	β- 100.00%	β- 100.00%
	β- = 1.00%		< 2.00%		β- 0.30%		
1040n 11.14n	1050n STABLE 22.25%	1060n STABLE 27.33%	1070n 4.52+0 Y	1080n STABLE 26.46%	1090n 13.70+2 E	1100n STABLE 11.72%	1110n 23.4 M
			β- 100.00%		β- 100.00%		β- 100.00%

Fig. 13 isotopes periodic table Pd,,Sn

One interesting intermediate state is ¹¹²In that has a more or less symmetric decay path either to ¹¹²Sn or ¹¹²Cd with a rate of about 2:1 in favor of Cd. The Q-value for ¹¹²Cd is much larger than for ¹¹²Sn which is one more a clear sign that the claimed original particle (n,p) mass does not explain the true nuclear structure. A stronger nuclear bond needs more internal charge to bind the added flux. As SOP shows the internal 2 rotation charge mass is around 2.36keV only which is far less than the electron mass or the neutrons excess mass.

5.4.1 The even chain





5.4.2 Intermediates lines of even chain

${}^{106}\text{Ag} :: 53.77 \rightarrow 113.88 \rightarrow 154.51 (\text{T } 361.9 \text{ T})$
 $\rightarrow 28.7 \rightarrow 95.28 \rightarrow 110.66$
 ${}^{106}\text{Ag} :: 414.9.4 (\text{T}) \rightarrow 153.8 (\text{T}) \rightarrow 158.5 \rightarrow$
 $95.28 (205.95 (\text{T})) \rightarrow 110.66$
 ${}^{106}\text{Ag} :: 511.9 (\text{decay line} - \text{low T})$
 ${}^{106}\text{Pd} :: 101 \rightarrow 616.174**** \rightarrow 511.85$
 ${}^{108}\text{Ag} :: 110.18 \rightarrow 113.6 (102.3) \rightarrow 329.2$
 $\rightarrow 46.44 ({}^{183}\text{W}!) (255.4 , 265.3) \rightarrow 30.33 \rightarrow$
 79.14
 ${}^{108}\text{Cd} :: 632.998 \rightarrow 0$
 ${}^{108}\text{Pd} :: 433.937 \rightarrow 0$
 ${}^{110}\text{In} :: 149.8 \rightarrow 56.4 \rightarrow 231.52 \rightarrow 100.0 \rightarrow$
 $131.28 \rightarrow 115.95 \rightarrow 118.8 (131.63) \rightarrow 140.3$
 (T)
 ${}^{110}\text{Ag} :: 406.3' \rightarrow 191.1 \rightarrow 51.2 \rightarrow 124.5 \rightarrow$
 116.48
 ${}^{110}\text{Ag} :: 182.7 \rightarrow 185.07 \rightarrow 79.85 \rightarrow 72.9 \rightarrow$
 $117.61 (\text{T})$
 ${}^{112}\text{Ag} :: \text{Not seen inside high background}$
 ${}^{112}\text{Pd} :: 291.6 \rightarrow 547 \rightarrow 373.8 (\text{T low})$
 ${}^{112}\text{Cd} :: 688.23 \rightarrow 120.68 \rightarrow 694.87 \rightarrow 617.518$
 keV
 ${}^{112}\text{In} :: 270.22 (\text{T}) \rightarrow 406.8 (\text{T}) \rightarrow 156.59$
 $(\text{exited state} \rightarrow {}^{112}\text{Sn}) - \text{decay } 617.5 \text{ very}$
 low.
 ${}^{112}\text{Sn} :: 401.3 (\text{T}') \rightarrow 203.2 \text{ only possible}$
 $\text{from } {}^{110}\text{Cd. Q-value } 665\text{keV from } {}^{112}\text{In is}$
 $\text{below first gamma state.}$
 ${}^{112}\text{Sn} :: 279.5 (470) \rightarrow 286$
 ${}^{112}\text{Sn} :: 234.8 \rightarrow$
 ${}^{114}\text{Sb} :: 234.9 (\text{T } 321.0 \rightarrow) \rightarrow 188.18 (90)$
 $\rightarrow 56.3 \rightarrow 27.33$
 ${}^{114}\text{In}/{}^{114}\text{Cd}:: 80.61 ({}^{166}\text{Er}?) \rightarrow 725.24 \rightarrow 558.43$
 $(\text{last two low above in many cases}).$
 ${}^{116}\text{In} :: 196.7 \rightarrow 157.0 \rightarrow 305.13 ({}^{166}\text{Er}) \rightarrow 82.3$
 $({}^{154}\text{Gd}) \rightarrow 112.5 \rightarrow 90.1 \rightarrow 96.1 (\text{T m})$

5.4.3 The odd chain

${}^{105}\text{Pd} + {}^2\text{H} \rightarrow {}^{107}\text{Ag} + {}^2\text{H} \rightarrow {}^{109}\text{Cd} \rightarrow {}^{109}\text{Ag} + {}^2\text{H} \rightarrow {}^{111}\text{Cd}$
 $+ {}^2\text{H} \rightarrow {}^{113}\text{Cd} + {}^2\text{H} \rightarrow {}^{115}\text{Sn}$
 effective reactions::
 ${}^{105}\text{Pd} + {}^2\text{H} \rightarrow {}^{107}\text{Cd} \rightarrow {}^{107}\text{Ag}$
 ${}^{109}\text{Ag} + {}^2\text{H} \rightarrow {}^{111}\text{In} \rightarrow {}^{111}\text{Cd}$

 ${}^{111}\text{Cd} + {}^2\text{H} \rightarrow {}^{113}\text{In} + {}^2\text{H} \rightarrow {}^{115}\text{Sn}$
 ${}^{113}\text{Cd} + {}^2\text{H} \rightarrow {}^{115}\text{In}$

For the above two paths we could not identify an intermediate isotope. ${}^{113}\text{In}$ is stable but has low spectral

visibility. Both stable Indium isotopes own a long living state which decouples cascading lines. So all lines we give for ${}^{113}\text{Cd}$ must come from adding H^*-H^* or a new high energy symmetric decay.

${}^{107}\text{Cd} :: 36.5 \rightarrow 303.53 \rightarrow 300.45 \rightarrow 204.98$
 $\text{keV} - \text{after magnetic } 845.54\text{keV state}$

${}^{107}\text{Cd} :: 640.58 \rightarrow 204.98 \text{ keV} - \text{after magnetic}$
 845.54keV state

${}^{109}\text{Cd} :: 259.7 \rightarrow 203.3 \text{ keV} - \text{after magnetic}$
 463.1keV state

${}^{111}\text{Cd} :: 203.29 \rightarrow 171.28 \rightarrow 245.39 \text{ keV} - \text{after}$
 $\text{magnetic } 416.72 \text{ keV state lower T. Final } 245.37 \text{ not seen}$
 $- \text{also in classical magnetic decay!}$

${}^{111}\text{In} :: 372.31 \rightarrow 325.5 \rightarrow 414.5 \rightarrow 265.7 \rightarrow$
 536.99keV

${}^{113}\text{Sn} :: 77.39\text{keV}$

${}^{113}\text{In} :: 689.5 \rightarrow 351.4 \rightarrow 382.9 \rightarrow$
 $255.14 (\text{T}) \rightarrow 391.7 (\text{long time magnetic!})$

${}^{113}\text{Cd} :: 356.7 (\text{t}), 369.1 (322.35 \text{ low}) \rightarrow$
 $96.9 ({}^{153}\text{Eu}?) \rightarrow 126 (\text{T}) \rightarrow 142.42 (\text{T}) (205.86)$
 $\rightarrow 17.78$

Fully connected magnetic lines $285.3 \rightarrow 298.6 \rightarrow 0!$

${}^{115}\text{In} :: 492.351 \rightarrow 336.241 \rightarrow 0 \text{ keV}$

${}^{115}\text{In} :: 231.443 \rightarrow 260.896 \text{ intermediate}$
 $\text{missing} \rightarrow 336.241 \rightarrow 497.334 \text{ keV } ({}^{115}\text{Sn}$
 $\text{decay lines!})$

336.241 is low as it is a slow state

${}^{115}\text{Sn } 497.334\text{keV}$ was high at a specific temperature and late in the experiment.

**** magnetic decay

In the Pd,...,Sn system we have a very high contribution by magnetic lines that most of the time are hidden I full down scaling paths exist. This will change in the next section.

6 The samarium complex

We here focus on a subset of the Nd \rightarrow Ho reaction chain. Inside this chain a new feature does occur. Many isotopes can undergo alpha decay. Even more exciting isotopes like ${}^{148}\text{Eu}$ can choose between alpha decay and beta (β^+) decay.

The tables in Fig. 14,15 below include about 30 "stable" isotopes. The magnetic elements Nd,Sm,Gd,Dy have been present from the beginning. Usually also traces of Europium and Terbium are present in magnetic powders. So here we can only show unstable intermediates and their decay path, that confirm an upscaling of mass. Even if we see an upscaling in the form $A(Z,N) + D^*-D^* \rightarrow A(Z+2, N+2)$ a followup decay can happen which gives a final reaction of:: $A(Z,N) + D^*-D^* \rightarrow A(Z+2, N+2) \rightarrow A(Z,N) + {}^4\text{He}$. We call this behavior a ${}^4\text{He}$ spallation reaction if the endpoint also shows a full downscaling from adding D^* .

Such ${}^4\text{He}$ spallation reactions are of greatest interest. If spallation dominates, then we will be able to build a long time stable Deuterium fusion reactor. If a LENR reaction does not consume = transmute the starting isotope then the fuel is left behind unchanged. Only energy will be

150.4 → 1660.0*****
¹⁴⁶Sm :: 251.2 → 234.9 (T 632!)
¹⁴⁶Sm :: 410.7 → 430.39 (low T) follow ups to low and
 high energy so no stop at ¹⁴⁶Sm.
¹⁴⁶Pm :: 462.8 → 135.6 → 93.8 (318.8 T) → 73.1
 Decay:: 453.8 (T)

¹⁴⁸Eu :: 666.9'' (454.2') → 90.7 (545.1''T) → 12.0***
 → 190.2 → (206.3 → 79.4) 285.7 → 232.8
 Also decay:: 550.2 553.2 (T)
¹⁴⁸Pm :: 288.11 → 311.57'T low. Also decay 550.27
 just once.
¹⁴⁸Pm :: 270.2 → 170.1 → (148.0 → low T) → 78.2 →
 62.2 (long living state)

¹⁵⁰Sm and ¹⁵²Sm see tables below
¹⁵²Gd :: 255.4 (overlapping) → 470.7 → 440.8 →
 471.98(M) → 411.12(M) → 344.28
¹⁵²Gd :: 255.4 → 470.7 → 440.8 → 385.9 → 159.16
 (172.1) → 192.6 → 175.9 → 411.12(M) → 344.28
¹⁵²Eu :: 304.5 → 290.5 → 276.5 → 258.25 → 238.48 →
 404.8 → 158.86 → 39.75 → 18.27*** → 89.65
¹⁵⁴Gd :: 225.3 → 203 → 180.3 → 155.6(T) → 144 → 219.6
 → 180.87 → 303.22 → 337.35 → 304.75 → 131.54 →
 180.72 → 134.82 → 557.58 → 123.07(T)
¹⁵⁶Gd :: 290.49 → 601.79 → 148.95 → 190.25 →
 79.88 → 960.50***** → 88.97
¹⁵⁶Gd :: 290.49 → 601.79 → 170.68 → 143.67 →
 104.55 → 960.50***** → 88.97

6.1.3 Odd lines paths

¹⁴³Nd + ²H → ¹⁴⁵Pm → ¹⁴⁵Nd + ²H → ¹⁴⁷Pm → ¹⁴⁷Sm
 → ¹⁴³Nd + ⁴He
¹⁴⁷Sm + ²H → ¹⁴⁹Eu → ¹⁴⁹Sm + ²H → ¹⁵¹Gd → ¹⁵¹Eu (→
¹⁵¹Sm) + ²H → ¹⁵³Gd → ¹⁵³Eu + ²H → ¹⁵⁵Tb → ¹⁵⁵Gd + ²H
 → ¹⁵⁷Gd
¹⁵¹Eu + ²H → ¹⁵³Gd + ²H → ¹⁵³Eu + ²H → ¹⁵⁵Tb → ¹⁵⁵Gd
 + ²H → ¹⁵⁷Gd

6.1.4 Comments odd lines

¹⁴⁵Nd + ²H □ ¹⁴⁷Pm □ ¹⁴⁷Sm □ ¹⁴³Nd + ⁴He likely!
 Most Nd lines have high energy.
¹⁴³Pm :: Evidence low.
¹⁵¹Eu :: Full downscaling seen up to 3,15 MeV! But low
 count numbers due to high energies.
¹⁵³Eu :: No spallation.

6.1.5 Odd Lines seen

¹⁴³Nd :: 152.0 → 546.6 → 563.8 low
¹⁴³Nd :: 275.6, 204.3 → 790.8*****
¹⁴³Nd :: 344.8 → 355.2 → 813.1*****
¹⁴⁵Nd :: 130.95(T) → 140.2(T) → 707.94'' (T) → 72.5
 (713.22'' T → 67.1)

¹⁴⁵Pm :: 410.4 (468.4 low) → 331(MT - 234.0 LT) →
 431.4 (492.55 HT) → 61.25
¹⁴⁹Pm :: 410.4 (468.4 low) → 163.3(153.87) → 168.04 →
 431.4 (492.55 HT) → 61.25
¹⁴⁷Pm :: 36.75 → 117.98 → 439.9 → 91.1
¹⁴⁷Sm :: 328.8 → 165.556 → 255,6 (244.8') →
 601.45(early low, late low 1T) → 76.07 → 121.22 (Q
 factor 2311keV)
¹⁴⁹Sm :: 130.1 → 178.58 → 327.52 (263.23(T),
 254.57(T) low) → 22.51
¹⁴⁹Sm :: 323.95 → 208.28 → 327.52 (263.23(T),
 254.57(T) low) → 22.51
¹⁴⁹Eu :: Decay:: 277.0, 178.58 → 327.53 → 22.51
¹⁵¹Gd :: 139.7 → 240.36 (275.61) → 236.14 (263.71 T)
 → 180.19 → 287.36 → 108.09 (HT)
 Decay:: 243.29, 153.6, 21.54 (¹⁵¹Eu)
¹⁵¹Eu :: 606.4 (T) → 561.5 → 431.9 → 59 → 463.7(T) →
 84 → 455 → 306 → 175 (196 → 0) → 21.54
¹⁵¹Eu :: 219.4 → 149.87 → 153.6 → 175 (196 → 0) →
 21.54
¹⁵¹Sm :: 307.5 → 527.6 → 273.2 → 247.8 → 105.7 →
 64.8 (69.7)
¹⁵¹Sm :: 217.31 (257.52'') → 143.2 (92.9'', 113.4) →
 134.88 → 62.8 → 35.13 → 69.7

In total more than 60 lines seen!

¹⁵³Eu :: 178.23 → 141.5'' (319.78) → 126.6 → 69.67 →
 19.81 → 83.37
¹⁵³Eu :: 141.54 → 126.67 → 96.88 → 69.67 → 19.81 →
 83.37
¹⁵³Gd :: 151.83 → 106.89 → 54.31(82,84,86.82,120.38)
 → 19.38 → 109.76
¹⁵³Gd :: 91.60 → 174.39 → 19.38 → 109.76
 Decay:: 97.43 (T), 103.18
 Decay X-ray :: 41.54,46.9x
¹⁵⁵Tb :: 439.7 (T) → 131.95 → 63.78 (181.5 T) →
 115.28 → 90.32 → 65.45 Decay 86.55, 105.32 (¹⁵⁵Gd)
 X-ray :: 43.0
¹⁵⁷Tb :: 182.4 (T) (233.7,281.8 T) → 83.04 → 60.88
 (¹⁵¹Sm overlapping)
¹⁵⁷Tb :: 153.3 (326.9 T) → 217.7 (222.2T) → 281.8
 (T) → 83.04 → 60.88
¹⁵⁹Tb 307.0 → 120.7 → 183.1 → 57.99
¹⁵⁹Tb 184.7 → 15.4*** → 290.3 → 57.99
¹⁶¹Dy 136.37 → 119.61 → 69.29 → 57.19 → 74.57 → 0
¹⁶¹Dy 101.99 → 138.39 → 74.57 → 0 (lesser)

6.2 ^4He spallation

The formation energy of ^4He from ^2H is $23'846'534.6\text{eV}$. If we add deuterium ($A + ^2\text{H}$) to a lower Z isotope, then we introduce up to 16 MeV of energy (e.g. Ni). Latest with Nd this changes to amounts between 9..12 MeV of excess energy in the target nucleus (A). If we can add $A + \text{D}^* - \text{D}^*$ then this usually adds less energy than the $\text{D}^* - \text{D}^* \rightarrow ^4\text{He}$ fusion would generate. So all reactions among isotopes (Fig.14, 15) that are close to the ^4He threshold show a very distinct behavior. Additional energy can be gained from ($A + ^2\text{H}$) reaction if in a follow reaction up ^4He spallation takes place.

Why do we say this? Our fuel mixture contains no Barium, a precursor for forming ^{140}Ce . But we can see several ^{140}Ce lines that only can be active if a high energy overloaded ^{144}Nd starts a ^4He spallation reaction that frees an additional about 1.9MeV carried back to ^{140}Ce . Interestingly enough the ^{140}Ce gamma orbit contain a $1'903\text{keV}$ state that more or less exactly matches the ^{144}Nd Q-value! tabulated as $1'901.3\text{keV}$. So these 2 nuclei are in close resonance according the above closed chain reaction.

Samarium (from mass 144 to 154) is a complex set of isotopes that spawns 6 “strong force quanta” (a basic SOP unity of mass released – about 10.845MeV - what also defines one basic SOP quantum number). Further Samarium lives in the center the periodic table where both decays beta +/- can be active in parallel. Even more interesting some reaction products of $\text{Sm} + ^2\text{H}$ ($^{148}\text{Sm} + 2\text{p} \rightarrow ^{150}\text{Gd}$) can undergo alpha decay which looks like 4-He spallation!

What we in fact did measure was not only the $^{150}\text{Sm} + 2\text{p} \rightarrow ^{152}\text{Gd}$ – see Fig 3. 271.1 keV line path, but also the parallel reaction line of $^{150}\text{Sm} + ^2\text{H} \rightarrow ^{152}\text{Eu}$. It looks like the endpoint ^{152}Gd is not stable due to the high excess energy (10.79MeV) that is well above the Q factor (2204.4keV) of ^{152}Gd . Further almost all lines end on the magnetic down scaling path from $1227.37 \rightarrow 755.396 \rightarrow 344.279\text{keV}$ path are seen. This last energy (344.279keV) of the non magnetic final state is high above background (Fig.3). Its a shared line with ^{183}W that has the same energy.

The ^{152}Eu 45.6keV line started to show up later in the experiment after about 5 hours!! (Half live 9.31h! of the excited 45.6keV isomer state that defines the beta +/- decay rate is also close/overlapping with X-rays – K-M_{1,2,3}) The interesting questions thus is: Is path 1) active because ^{152}Gd can efficiently downscale excess energy or because the isomer state of ^{152}Eu blocks the down-scaling?

The $^{148}\text{Sm} \rightarrow ^{152}\text{Sm}$ path is able to produce $21'697'502.5\text{eV}$
The $^{148}\text{Sm} \rightarrow ^{152}\text{Eu}$ path is able to produce $19'823'192.0\text{eV}$

In both isotopes ^{148}Sm and ^{152}Sm we see many lines above the downscaling threshold and also above the spallation threshold, that would be $23'846'534.6\text{eV}$ for D-D fusion – e.g. $21'697'502.5\text{eV}$ which is about 2.15MeV (starting from stable isotope). Interesting is that fully connected decays for ^{152}Sm are laying inside the spallation threshold

(2.15MeV). In the tables below orange lines are clearly seen, where as blue means seen to barely seen (light blue). This is for a single spectrum at the most active point. In case of ^{152}Sm most energies seen above the spallation threshold are not connected (black is a dead end light blue most likely too.) or only weekly (blue).

Advanced SOP alpha wave modeling shows that ^{152}Sm can maximally accept about 5MeV, thats also where the known spectrum ends. For ^{150}Sm its only about 2.4MeV. These thresholds do affect the internal stability.

The other fact is that we see multiple parallel excitation paths. Energetically the formation of ^4He out of D-D is always favorable. This is not the case for Pd – Ag – Cd cycle! So there is a high chance that the overloading of ^{150}Sm or ^{152}Sm leads to the spallation of ^4He . This would transform them back to ^{146}Sm or ^{148}Sm . For all the reaction steps between ^{146}Sm and ^{152}Sm we see the unstable intermediates (^{150}Eu , ^{152}Eu) what confirms that the upward chain is running.

Of course almost all the lines below cannot be triggered by magnetic downscaling too. The most likely reason is a spallation reaction as adding as single deuterium (+ about 11 MeV) is not covered by the known gamma spectrum. So this is the most important finding of our research.

We will stop here as this would not add more basic knowledge. The next isotope that shows a broad spectral response is ^{156}Gd . Not so for ^{154}Sm or ^{154}Gd . So we can only note that we did see different spallation hot spots and that cold fusion - most likely - is able to produce all known elements just by adding Hydrogen and follow up decays.

The observed ^4He spallation in **rare earths** could also explain why we have to call them rare!

Rare is a relative term. Rare earths are not particularly rare, as compared to gold for example, just expensive to extract in pure form

Magnetic decay	state	target state	line energy
M1,M2	121.7818	0	121.7817
M1,M2	366.4793	121.7818	244.6974
	684.751	121.7818	562.98
	684.751	0	684.85
M1	706.928	366.4793	340.45
M2	810.453	684.751	125.64
M2	810.453	366.4793	444
M2	810.453	121.7818	688.67
M2	810.453	0	810.451
	963.358	810.453	152.77
	963.358	684.751	278.7
	1022.97	810.453	212.43
	1082.842	963.358	119.46
	1082.842	810.453	272.41
M2	1085.841	810.453	275.41
M1	1125.39	706.928	418.45
	1221.64	706.928	514.78
	1233.863	1022.97	210.95
	1292.773	1082.842	209.97
	1292.773	963.358	329.436
	1310.505	1221.64	89.17
	1371.735	1233.863	137.56
	1371.735	1221.64	150.13
	1371.735	1085.841	285.84
	1371.735	1022.97	348.751
	1510.79	1292.773	218.1
	1510.79	1082.842	427.9
	1510.79	1041.122	469.97
?	1529.802	1292.773	237.11
?	1529.802	1233.863	295.9387
?	1529.802	1085.841	443.9606
?	1529.802	963.358	566.438
	1559.62	1233.863	325.69
T	1579.429	1371.735	207.64
T	1579.429	1292.773	286.5
T	1579.429	1085.841	493.54
T	1579.429	1022.97	556.48
M1	1609.26	1125.39	483.86
	1612.9	1292.773	320.1
	1612.9	1233.863	379.05
	1612.9	1221.64	391.19
	1612.9	1085.841	527.1
	1612.9	810.453	802
	1649.831	1292.773	357.26
	1649.831	1233.863	416.02
	1666.45	1505.77	160.8
	1666.45	1310.505	355.9
	1680.56	1085.841	594.7
	1728.27	1505.77	222.89

Magnetic decay	state	target state	line energy
	1728.27	1371.735	356.56
	1728.27	1221.64	506.6
T	1730.205	1371.735	358.48
T	1754.98	1292.773	462.16
T	1769.132	1292.773	476.43
	1803.94	1371.735	432.1
	1803.94	366.4793	1437.5
	1879.14	1609.26	269.8
	1879.14	1505.77	373.7
	1891.06	1757.001	134.73
	1891.06	1371.735	519.9
T	1906.13	1649.831	255.96
	1920.46	1803.94	116.51
	1929.93	1559.62	370.24
	1945.9	1728.27	217.6
T	1977.19	1310.505	667.5
T	2040.09	1891.06	149.06
T	2040.09	1757.001	283.94
T	2040.09	1728.27	312
T	2040.09	1612.9	427
	2057.52	1803.94	253.2
	2057.52	1728.27	329.4
T	2069.31	1680.56	388.75
	2079.57	1879.14	200.52
	2079.57	1666.45	413.11
	2079.57	1609.26	470.36
T	2096.82	1371.735	725.13
	2120.98	2057.52	63.51
	2120.98	1920.46	200.6
T	2127.17	1510.79	616
	2139.71	1728.27	411.65
	2201.47	1879.14	322.2
T	2206	1945.9	260
T	2206	1929.93	276
T	2206	1728.27	478
	2214.98	1945.9	269
	2214.98	1920.46	294.4
	2269.87	2120.98	148.95
	2320.35	1803.94	516.3
	2375.49	2139.71	235.8
	2388.79	2214.98	173.8
	2388.79	2201.47	187.6
	2388.79	2057.52	331.3
	2424.36	2269.87	154.6
	2424.36	2120.98	303.5
	2445.9	1879.14	567.1
	2510.59	2375.49	135.13
	2525.69	2326.94	198.83
	2576.29	2424.36	152.1
	2576.29	2388.79	187.6
	2641.09	2148.81	493
	2641.09	2079.57	560.9

Fig. 16 Gamma lines energies seen for ¹⁵²Sm marked with follow up lines at 388C

upper part Fig.16

Magnetic decay	state	target state	line energy
M	333.955	0	333.961
	740.464	333.955	406.508
M	773.374	333.955	439.4
M	1046.148	740.464	305.68
	1071.406	333.955	737.457
	1165.791	740.464	425.22
M	1193.843	1046.148	147.73
(T°)	1255.512	740.464	515.3
	1255.512	333.955	921.55
M	1278.922	773.374	505.508
	1357.71	1278.922	78.76
	1357.71	1071.406	286.29
	1417.346	1255.512	161.84
	1417.346	1193.843	223.51
	1417.346	1165.791	251.582
	1449.182	1278.922	170.23
	1504.572	1193.843	310.75
	1642.611	1504.572	138.05
	1642.611	1449.182	193.46
	1642.611	1417.346	225.34
	1658.39	1165.791	492.53
	1684.162	740.464	944
	1713.51	1165.791	548.59
	1713.51	1046.148	667.31
	1760.06	1642.611	117.58
T	1821.894	1642.611	179.26
T	1821.894	1278.922	542.97
	1822.472	773.374	1049.04
	1833.01	1165.791	667.05
	1837.03	1278.922	558.1
	1952.46	1642.611	308.05
	1970.465	1684.162	286.29
T	2024.663	1357.71	667.05
	2070.27	1504.572	565.7

Magnetic decay	state	target state	line energy
	2070.27	1417.346	652.84
	2070.27	1165.791	904.46
T	2095.33	1970.465	125
T	2095.33	1822.472	272.82
T	2095.33	1760.06	335.7
T	2095.33	1504.572	590.79
T	2117.03	1449.182	667.05
T ¹⁴⁷ Sm	2119.36	1833.01	286.29
T	2119.36	1642.611	476.89
T ¹⁵¹ Sm	2193.51	1952.46	240.03
	2232.37	1837.03	395.1
	2433.19	2232.37	200.6
T	2602.5	1713.51	889.2
(T° low)	2744.35	2232.37	512
	2929.24	2433.19	495.8
T ^{(150)SM}	2995.9	2744.35	251.6
T	2995.9	2232.37	763.5
T	3038.2	2812.88	225
T	3050	2550.57	499.4
T	3050	2507.27	542.9
T	3089.4	2812.88	276.5
	3293.3	3048.4	244.7
	3384.2	3048.4	335.9
	3384.2	2929.24	454.8
	3675.9	3293.3	382.4
	3914.1	3675.9	238.3
	3941.2	3384.2	557
	4025.2	3835	190.1
	4025.2	3522.7	502.5
	4305.8	3835	470.5
	4386.3	3914.1	472.2
T	4386.3	3835	551.2
	4576.2	3941.2	635
T	4929.1	4386.3	542.7

Fig. 17 Gamma lines energies seen for ¹⁵⁰Sm marked T terminal, M magnetic, "orange" high above background, upper part Fig.17

7 Summary

We here did show the results of a cold fusion experiment made with Deuterium loaded powders consisting of stable rare earth and magnetic elements. Obviously it was possible to start a large number of new type (cold fusion) nuclear reactions. This could be proven by analyzing 10 gamma spectra from a highly activated fuel. We could identify several hundred lines and long cascading decays. This experiment will deeply change a part of descriptive physics that so far lacks any logical explanation. The experiment shows that in the investigated region of the periodic table all elements can be produced just by adding Hydrogen.

Samarium shows a very interesting behavior, that possibly could be exploited for a stable energy production device. As the starting isotopes are reproduced after ^4He spallation one can assume that under ideal conditions only the $2\ ^2\text{H} \rightarrow\ ^4\text{He}$ reaction runs.

^4He spallation also explains why rare earth are rare because starting with cerium the build up is slowed down.

8 Outlook

In a future experiment we plan to use the gained knowledge to make cold fusion power cells more reproducible. By narrowing the broad set of elements used to the potentially necessary ones we, hope to get more clear signals and also a better understanding of the temperature dependency of the reactions.

[1] Fleischmann, M., S. Pons, and M. Hawkins, Electrochemically induced nuclear fusion of deuterium. *J. Electroanal. Chem.*, 1989.

[2] Ruggerio M. Santilli , A new gaseous and combustible form of water, *International Journal of Hydrogen Energy*, <https://doi.org/10.1016/j.ijhydene.2005.11.006>

[3] Leif Holmlid, Mesons from Laser-Induced Processes in Ultra-Dense Hydrogen H(0), *PLOS one* doi:10.1371/

[4] Leif Holmlid, Leptons from decay of mesons in the laser-induced particle pulse from ultra-dense protium p(0), *International Journal of Modern Physics E* Vol. 25 No. 10 (2016) DOI: 10.1142/S0218301316500853

[5] H. Fukuoka, T. Ikegawa t, K. Kobayashi:, A. Takahashi, Osaka University, Measurement of excess heat and nuclear products in PD-D2O Systems using twin open type electrolysis cells, Department of Nuclear Engineering, ICCF-6 proceedings October 1 J-18, 1996 japan (<https://lenr-canr.org/acrobat/NEDOthesixthina.pdf#page=24>)

[6] R.Mills Brilliant power Analytical_Presentation 1. March, 2019

[7] J. A. Wyttenbach, independent researcher, The proton, electron structure, its resonances and fusion products, Researchgate, 2021

[8] Roger Stringham, John Chandler, Russ George, Tom Passell, and Richard Raymond, First Gate Energies, Mountain View, CA, USA, PREDICT ABLE AND REPRODUCIBLE HEAT, ICCF-7 proceedings, Vancouver, 1998

[9] Passell, T.O. and R. George. Trace Elements Added to Palladium by Exposure to Gaseous Deuterium. in 8th (<https://lenr-canr.org/acrobat/PassellTOtraceleme.pdf>)

International Conference on Cold Fusion. 2000. Lerici (La Spezia)

[10] IAEA online nuclear data pages <https://www-nds.iaea.org/relnsd/vcharthtml/VChartHTML.html>

[11] S. Focardi, V. Gabbani, V. Montalbano , F. Piantelli and S. Veronesi , Evidence of electromagnetic radiation from Ni-H Systems

Proceedings of Eleventh International Conference on Condensed Matter Nuclear Science. 2004. Marseille, France.

[12] Leif Holmlid ,Time-of-flight of He ions from laser-induced processes in ultra-dense deuterium D(0), Atmospheric Science, Department of Chemistry and Molecular Biology, University of Gothenburg , *International Journal of mass spectrometry* , 2014

[13] A. Klimov, A. Grigorenko, A. Efimov, N. Evstigneev, O. Ryabkov, M. Sidorenko, A. Soloviev and B. Tolkunov,High-energetic Nano-cluster Plasmod and its Soft X-ray Radiation, *J. Condensed Matter Nucl. Sci.* 19 (2016) 145–154

[14] J. A. Wyttenbach, independent researcher, Method for enabling low energy nuclear reactions by the Rotator Collapse Field-Coupled (RCFC) effect, US patent application application 15/444,580 2018

[15] P.L. Hagelstein,, Massachusetts Institute of Technology, Cambridge, MA, USA, Phonon-mediated Nuclear Excitation Transfer, *Journal of Condensed Matter Nuclear Science* 27 (2018) 97–142

[16] 2016: Mills, Randell L., *The GRAND UNIFIED THEORY of CLASSICAL QUANTUM MECHANICS*;ISBN 978-0-9635171-5-9 (2016) online.

[17] F. Ghabussi, University of Konstanz, Topological aspects of WKB method, Researchgate 2021

[18] A. A. Kazhymurat. On a lower bound for the energy functional on a family of Hamiltonian minimal Lagrangian tori in CP 2

arXiv:1710.00322.pdf, 29 September 2017

[19] G. Sardin, University of Barcelona, About the symmetry of the deuteron structural charge density distribution <https://www.researchgate.net/publication/330825167>, Februar 2019

[20] J. A. Wyttenbach, Nuclear & Particle Physics version 2.0; Main achievements < SO(4) physics >, Researchgate, 2019

[21] J.A.Wyttenbach, NPP 2.1, researchgate, (2018, online),

under <https://www.researchgate.net/project/Nuclear-and-particle-physics-20>

[22] M. Swartz, Atomic deuterium in active LANR systems produce 327.37 MHz Superhyperfine RF MASER emission, ICCF-22

Abstract, Sept. 2019.

[23] Lipinski WO2014189799 united gravity about LiP (H*) fusion.